Supporting Information.....

Table S1: qPCR data analysis of *ACO1*

Average Experimental Ct Value TE	Average Experimental Ct Value HE	Average Contrl Ct Value TC	Average Contrl Ct Value HC
29.55	21.73	29.65	21.56

ΔCt Value (Experimental/ ΔCTE) = TE-HE = 7.82

ΔCt Value (Control/ ΔCTC) = TC-HC = 8.09

ΔΔCt value = ΔCTE- ΔCTC = -0.27

Fold change = $2^{-\Delta\Delta Ct}$ = 1.2

Gene being Tested Experimental (TE): *ACO1* Stress

Gene being Tested Control (TC): *ACO1* Control

Housekeeping Gene Experimental (HE): *GAPDH* Stress

Housekeeping Gene Control (HC): *GAPDH* Control

Table S2: qPCR data analysis of *ACO2*

Average Experimental Ct Value TE	Average Experimental Ct Value HE	Average Control Ct Value TC	Average Control Ct Value HC
29.42	21.58	28.55	21.87

ΔCt Value (Experimental/ ΔCTE) = TE-HE = 7.84

ΔCt Value (Control/ ΔCTC) = TC-HC = 6.68

ΔΔCt value = ΔCTE- ΔCTC = 1.16

Fold change = $2^{-\Delta\Delta Ct}$ = 0.45

Gene being Tested Experimental (TE): *ACO2* Stress

Gene being Tested Control (TC): *ACO2* Control

Housekeeping Gene Experimental (HE): *GAPDH* Stress

Housekeeping Gene Control (HC): *GAPDH* Control

Table S3: qPCR data analysis of *ADH1*

Average Experimental Ct Value TE	Average Experimental Ct Value HE	Average Contrl Ct Value TC	Average Contrl Ct Value HC
24.175	18.01	25.84	18.565

ΔCt Value (Experimental/ ΔCTE) = TE-HE = 6.165

ΔCt Value (Control/ ΔCTC) = TC-HC = 7.275

ΔΔCt value = ΔCTE- ΔCTC = -1.11

Fold change = 2 -ΔΔCt = 2.16

Gene being Tested Experimental (TE): *ADH1* Stress

Gene being Tested Control (TC): *ADH1* Control

Housekeeping Gene Experimental (HE): *GAPDH* Stress

Housekeeping Gene Control (HC): *GAPDH* Control

Table S4: qPCR data analysis of *ADH2*

Average Experimental Ct Value TE	Average Experimental Ct Value HE	Average Control Ct Value TC	Average Control Ct Value HC
24.53	18.01	26.355	18.565

ΔCt Value (Experimental/ ΔCTE) = TE-HE = 6.52

ΔCt Value (Control/ ΔCTC) = TC-HC = 7.79

ΔΔCt value = ΔCTE- ΔCTC = -1.27

Fold change = 2 -ΔΔCt = 2.41

Gene being Tested Experimental (TE): *ADH2* Stress

Gene being Tested Control (TC): *ADH2* Control

Housekeeping Gene Experimental (HE): *GAPDH* Stress

Housekeeping Gene Control (HC): *GAPDH* Control

Table S5: qPCR data analysis of *ADH3*

Average Experimental Ct Value TE	Average Experimental Ct Value HE	Average Control Ct Value TC	Average Control Ct Value HC
19.49	18.42	21.17	18.31

ΔCt Value (Experimental/ ΔCTE) = TE-HE = 1.07

ΔCt Value (Control/ ΔCTC) = TC-HC = 2.86

ΔΔCt value = ΔCTE- ΔCTC = -1.79

Fold change = 2 -ΔΔCt = 3.46

Gene being Tested Experimental (TE): *ADH3* Stress

Gene being Tested Control (TC): *ADH3* Control

Housekeeping Gene Experimental (HE): *GAPDH* Stress

Housekeeping Gene Control (HC): *GAPDH* Control

Table S6: qPCR data analysis of *ADH1*

Average Experimental Ct Value TE	Average Experimental Ct Value HE	Average Contrl Ct Value TC	Average Contrl Ct Value HC
21.65	18.2	22.04	18.47

ΔCt Value (Experimental/ ΔCTE) = TE-HE = 3.47

ΔCt Value (Control/ ΔCTC) = TC-HC = 3.57

ΔΔCt value = ΔCTE- ΔCTC = 0.1

Fold change = $2^{-\Delta\Delta Ct}$ = 1.07

Gene being Tested Experimental (TE): *ADH1* Stress

Gene being Tested Control (TC): *ADH1* Control

Housekeeping Gene Experimental (HE): *GAPDH* Stress

Housekeeping Gene Control (HC): *GAPDH* Control

Table S7: qPCR data analysis of *ADH2*

Average Experimental Ct Value TE	Average Experimental Ct Value HE	Average Contrl Ct Value TC	Average Contrl Ct Value HC
25.975	18.2	26.35	18.47

ΔCt Value (Experimental/ ΔCTE) = TE-HE = 7.775

ΔCt Value (Control/ ΔCTC) = TC-HC = 7.88

ΔΔCt value = ΔCTE- ΔCTC = -0.105

Fold change = $2^{-\Delta\Delta Ct}$ = 1.08

Gene being Tested Experimental (TE): *ADH2* Stress

Gene being Tested Control (TC): *ADH2* Control

Housekeeping Gene Experimental (HE): *GAPDH* Stress

Housekeeping Gene Control (HC): *GAPDH* Control

Table S8: qPCR data analysis of *ADH3*

Average Experimental Ct Value TE	Average Experimental Ct Value HE	Average Contrl Ct Value TC	Average Contrl Ct Value HC
21.935	23.43	24.135	23.595

ΔCt Value (Experimental/ ΔCTE) = TE-HE = -1.495

ΔCt Value (Control/ ΔCTC) = TC-HC = 0.54

ΔΔCt value = ΔCTE- ΔCTC = -2.035

Fold change = $2^{-\Delta\Delta Ct}$ = 4.098

Gene being Tested Experimental (TE): *ADH3* Stress

Gene being Tested Control (TC): *ADH3* Control

Housekeeping Gene Experimental (HE): *GAPDH* Stress

Housekeeping Gene Control (HC): *GAPDH* Control

Table S9: Citrate content in treated and control (untreated) culture of *S. cerevisiae*

Sample	Extracellular citrate content (ng/µL)	Intracellular citrate content (ng/µL)	Total citrate content (ng/µL)
Control	29±3	13±2	42±3
Treated	15±2	6±NA	21±2

Abbreviations...

ACO: Aconitase

AD: Alzheimer's disease

ADH: Alcohol dehydrogenase

$AgNO_3$: Silver nitrate

ALDH: Aldehyde dehydrogenase

ALS: Amyotrophic lateral sclerosis

ANOVA: Analysis of variance

Arg: Arginine

AsA: Ascorbate

Bax: Bcl-2-associated X *protein*

bcl-2: B-cell lymphoma 2

BH_4: Tetrahydrobiopterin

BK: Bradykinin

bNOS: bacterial NOS

BP: Biological process

BSA: *Bovine serum albumin*

Ca^{2+}: Calcium

CaM: Calmodulin

cAMP: cyclic adenosine monophosphate

Cav-1: Caveolin-1

CBF: Cerebral blood flow

CC: Cellular component

C*c*O: cytochrome *c* oxidase

CCRD-RSM: Central Composite Rotational Design- Response Surface Model

cDNA: Complementary DNA

CFE: Cell-free extract

cGMP: cyclic guanosine monophosphate

cIMP: cyclic inosine monophosphate

CLS: Chronological life span

CO_2: Carbondioxide

CS: Citrate synthase

CTAB: cetyltrimethylammonium bromide

Cys: Cysteine

DAF-FM:4-Amino-5-Methylamino-2',7'-Difluorofluorescein Diacetate

DAVID: Database for Annotation, Visualization and Integrated Discovery

DdH_2O: Double distilled water

DetaNONOate: Diethylenetriamine NONOate

DHLA: Dihydro lipoic acid

DNS: 3,5-Dinitrosalicylic acid

DR: Dietary restriction

DTNB: 5,5'-dithio-bis-(2-nitrobenzoic acid)

EDTA: Ethylenediaminetetraacetic acid

EDRF: Endothelium-derived relaxing factor

eNOS: Endothelial nitric oxide synthase

ERK: Extracellular signal-regulated kinases

ETC: Electron transport chain

FACS: Fluorescence-activated cell sorting

FAD: Flavin Adenine Dinucleotide

Fe: Iron

FITC: Fluorescein isothiocyanate

FMN: Flavin Mono-Nucleotide

GAPDH: Glyceraldehyde-3-phosphate dehydrogenase

GCL: γ-glutamylcysteine ligase

GO: Gene Ontology

GPCR: G-protein coupled receptor

GPx: Glutathione peroxidase

GR: Glutathione reductase

GRK2: G-protein coupled receptor kinase 2

GS-FDH: GSH-dependent formaldehyde dehydrogenase

GS: GSH synthetase

GSH: reduced glutathione

GSNO: *S*-nitrosoglutathione

GSNOR: GSNO reductase

GSSG: oxidized glutathione

h: Hour

$HCLO_4$: Perchloric acid

HD: Huntington's disease

HDAC2: Histone Deacetylase 2

H_2DCFDA: 2′,7′-Dichlorodihydrofluorescein diacetate

HEPES: 4-(2-hydroxyethyl)-1-piperazineethanesulfonic acid

Hmp1: Flavohemoprotein

HNE: 4-hydroxy-2-nonenal

H_2O_2: Hydrogen peroxide

H_2ONO^+: nitrous acidium ion

HRP: Horseradish peroxidase

H_2SO_4: Sulfuric acid

hsp90: Heat shock protein 90

ICDH: Isocitrate dehydrogenase

ICL: Isocitrate lyase

iNOS: Inducible nitric oxide synthase

InsP3RI: Inositol-1,4,5-trisphosphate receptor type I

iodoTMT: Iodoacetyl Tandem Mass Tags

IRAG: Inositol-1,4,5-triphosphate receptor associated cGMP kinase substrate

JNK: c-Jun N-terminal kinase

KCl: Potassium Chloride

$K_2Cr_2O_7$: Potassium dichromate

KMnO4: Potassium permanganate

KOH: Potassium hydroxide

LA: Lipoic acid

LDL: Low density lipoprotein

Leu: Leucine

L-NNA: NG-nitro-L-arginine

L-NAME: NG-Nitro- L-Arginine Methyl Ester

LOONO: Peroxynitrite intermediates

M: Molar

MAPK: Mitogen-activated protein kinase

MDA: Monodehydroascorbate

MDH: Malate dehydrogenase

MDH (DC): Malate dehydrogenase (decarboxylating)

MF: Molecular function

MLCK: Myosin light chain kinase

MLCP: Myosin light chain phosphatase

mM: milli-molar

MMTS: *S*- methyl methanethiosulfonate

MOPS: 3-(N-morpholino)propanesulfonic acid

MRC: mitochondrial respiratory chain complex

MRSA: methicillin resistance *Staphylococcus aureus*

mtDNA: Mitochondrial DNA

N: Nitrogen

NaCl: Sodium chloride

NAD: Nicotinamide adenine dinucleotide

NADH: Nicotinamide adenine dinucleotide hydrogen

NADPH: Nicotinamide adenine dinucleotide phosphate hydrogen

$NaNO_2$: acidified sodium nitrite

NHA: Nω-hydroxy-L-arginine

nNOS: Neuronal nitric oxide synthase

NO: Nitric oxide

NO^+: nitrosonium ion

NO_2: Nitrogen dioxide

NO_2^-: Nitrite

NO_3^-: Nitrate

NOS: Nitric oxide synthase

N_2O_3: dinitrogen trioxide

NOD: Nitric oxide dioxygenase

NOSIP: Nitric oxide synthase interacting protein

NOSTRIN: nitric oxide synthase trafficking inducer

O_2: Oxygen

O_2^-: Superoxide

OAA: Oxaloacetic acid

O.D.: Optical density

$ONOO^-$: Peroxynitrite

ORF: Open reading frame

PAGE*:* Polyacrylamide gel electrophoresis

PARP: Poly ADP-ribose polymerase

PBS: Phosphate-buffered saline

PC: Pyruvate carboxylase

PD: Parkinson's disease

PDC: Pyruvate decarboxylase

PDH: Pyruvate dehydrogenase

PDZ: post-synaptic density protein, discs-large, zona occludens -1

Phe: Phenylalanine

PKA: *Protein* kinase A

PKC: Protein kinase C

PM: Plasma membrane

PMSF: phenylmethylsulfonyl fluoride

polyQ: Polyglutamine

PTN: Protein tyrosine nitration

PTP: Permeability transition pore

PVDF: polyvinylidene difluoride

R^2: coefficient of determination

rDNA: Ribosomal DNA

RLS: Replicative life span

RNS: Reactive nitrogen species

ROS: Reactive oxygen species

$RS^{\bullet}$: Thiyl radical

RSNO: S-nitrosothiols

SD: Standard deviation

SDS: Sodium dodecyl sulphate

Ser: Serine

SERCA: Sarco/endoplasmic reticulum calcium ATPase

sGC: soluble guanylate cyclase

SR: sarcoplasmic reticulum

STRING: Search Tool for the Retrieval of Interacting Genes/Proteins

STREP: stress-starvation response element of *Schizosaccharomyces pombe*

TBST buffer: Tris buffered saline tween

TCA: tricarboxylic acid

Thr: Threonine

TRADD: TNF-receptor associated death domain protein

TRP: Transient receptor potential

Tyr: Tyrosine

VASP: Vasodilator sensitive phosphoprotein

VDCC: Voltage-dependent calcium channel

VLCAD: very long-chain acyl-CoA dehydrogenase

XOR: Xanthine oxidoreductase

Yhb1: Flavohemoglobin

YPD: yeast extract, peptone, dextrose

Zn: Zinc

Publications...

Cell Biochemistry and Biophysics (2020) 78:101–110
https://doi.org/10.1007/s12013-019-00897-y

ORIGINAL PAPER

Check for updates

Optimization of Ethanol Production using Nitrosative Stress Exposed *S.cerevisiae*

Swarnab Sengupta[1] · Minakshi Deb[1] · Rohan Nath[1] · Shyama Prasad Saha[1] · Arindam Bhattacharjee[1]

Received: 24 July 2019 / Accepted: 12 December 2019 / Published online: 24 December 2019

Abstract
S.cerevisiae is an industrially important organism known for its ability to produce ethanol as the demand for ethanol is increasing day by day all over the world, the need to find better and alternative ways to increase ethanol production is also rising. In this work we have proposed such alternative but effective method for producing ethanol by *S.cerevisiae*. Here, we are reporting for the first time the effect of nitrosative stress on ethanol production. Under in vivo condition, nitrosative stress is marked by the modification of macromolecules in the presence of reactive nitrogen species (RNS). Our result showed that treated cells were more capable for ethanol production compared with untreated cells. Our result also showed enhanced alcohol dehydrogenase activity under stressed condition. Further ethanol production was also optimized by using Response Surface Methodology (RSM) with stressed cells. Further, production of ethanol with immobilized beads of stress affected *Saccharomyces cerevisiae* was also determined. Overall, the obtained data showed that under nitrosative stress, the maximum ethanol production is 34.4 g/l after 24 h and such higher production was observed even after several cycles of fermentation. This is the first report of this kind showing the relation between nitrosative stress and ethanol production in *Saccharomyces cerevisiae* which may have important industrial application.

Keywords *Saccharomyces cerevisiae* · Nitrosative stress · Reactive nitrogen species (RNS) · Response surface methodology (RSM).

Introduction

Demand for ethanol is increasing day by day due to its versatile application and utility. To meet the acting demands, production of ethyl alcohol or ethanol through fermentation is gaining momentum globally. Despite the evolving trend of using bacteria for ethanol production, yeast is still the primary choice for fermentation [1]. Due to its high ethanol productivity, high ethanol tolerance and ability of fermenting wide range of sugars, yeasts especially *Saccharomyces cerevisiae* is the common microorganism employed in ethanol production [2]. In recent years, different strains of *Saccharomyces cerevisiae* were extensively studied to improve their ability for ethanol production. Industrially engineered yeast strains have to resist to the stress conditions rapidly and they have to adapt quickly by modifying their metabolic activities to avoid substantial viability loss. Ethanol production by using immobilized cells also has significant advances. Immobilized cells offer rapid fermentation rates with high productivity of ethanol. Immobilization enhances ethanol productivity and its yield while at the same time effectively eliminate the obstacles caused by high concentration of substrate and product in ethanol production. Hence the technique holds a great promise for the efficient production of fermented beverages, such as beer, wine as well as bioethanol [3].

Through metabolic engineering, bacterial and yeast strains have been constructed, which feature traits that are advantageous for ethanol production using lignocellulosic sugars [4]. But on the other hand, the inserted genes may have unexpected harmful effects. Another difficulty particular to the food and beverage industry is that containment of engineered yeast within the industrial plant cannot be guaranteed. Engineered yeast strains used in food and beverage production could be consumed by humans and may be released to the environment [5]. Moreover, metabolic and genetic engineering processes are highly

✉ Arindam Bhattacharjee
arbiochem@gmail.com

[1] Department of Microbiology, University of North Bengal, Siliguri, India

expensive, which is proving to be disadvantageous for the industries. To avoid such hurdles, new and cost effective alternative methods are needed. This work mainly focuses on proposing one such approach to increase ethanol production by applying nitrosative stress on yeast cells. Yeast cells can sense and adapt their physiology to the sequential stress conditions that they encounter. Therefore increasing stress tolerance is a suitable way to improve yeast industrial tolerance [6, 7].

In cell biology, "Stress" is a general term used to signify an event where under in vivo conditions the biochemical redox homeostasis of a cell is changed due to excessive production of different reactive species because of external stimuli, for e.g., the production of ROS (reactive oxygen species) and RNS (reactive nitrogen species). When a cell is challenged with RNS such as nitric oxide radical, peroxynitrite, nitrogen oxide radicals [8, 9], the hostile condition is known as "Nitrosative stress". In this stress condition an imbalance in the production and neutralization of reactive nitrogen and oxygen species, results in cellular damage [10]. RNS is formed due to the reaction of ROS and nitric oxide (NO). NO is a freely diffusible, short lived, and lipophilic molecule [11]. This agent acts as a key element of nitrosative stress in higher concentration. At this high concentration, it is actually toxic to cell as it can bind to heme, iron and copper containing protein [12, 13]. RNS can cause nitrosylation or nitration of different cellular components including metals, lipids, DNA, proteins which may inhibit or alter normal physiological functions [13]. It has been reported that several proteins of aerobic respiration e.g. aconitase, isocitrate dehydrogenase etc, can be nitrated that may result in the inhibition of TCA cycle in *Saccharomyces cerevisiae* [14]. It has been reported previously that the key enzyme of ethanol fermentation i.e. alcohol dehydrogenase of *Saccharomyces cerevisiae* can be affected during nitrosative stress [15]. Studies also suggest that when cells are exposed to nitrosative stress, intracellular redox homeostasis gets altered. This changed redox environment may lead to alteration in the physiochemical properties of the cell. Under such circumstances some proteins known as stress response enzymes, gets activated [16]. In this circumstance, it can be assumed that the metabolic pathway of *Saccharomyces cerevisiae* can be affected under nitrosative stress. Hence, the shifting of metabolic flux towards ethanol production becomes the study of interest. But there is almost no work in this field. On the other hand, it has also been reported that ethanol can be produced by *Saccharomyces cerevisiae* in both aerobic and anaerobic conditions [17].

Hence, the primary aim of this work was to study the effect of nitrosative stress on ethanol production by *Saccharomyces cerevisiae* in non-fermentative condition. The ethanol production by the immobilized nitrated yeast cells in a cheap medium containing molasses as the only carbon source was also an important objective of this study. This study will set up an approach that can be widely used in industry for higher alcohol production at low cost.

Materials and Methods

Yeast Culture and Growth Condition

Wild type haploid yeast cell *Saccharomyces cerevisiae* Y190 [ATCC 96400], a gift from Prof. Sanjay Ghosh, CU, was used for all experimental purpose. To grow, yeast culture was maintained at 30 °C temperature in shaking condition (80 rpm) in YPD (2% W\V Yeast extract, 2% W \V peptone, and 2% W\V dextrose) medium and YPG medium (2% W\V yeast extract, 2% W\V peptone, and 3% V/V glycerol) for all our experimental conditions. Molasses and ammonium sulfate containing medium was used for the experiment based on CCRD-RSM. Acidified sodium nitrite was used as the stress agent for all the experiment.

Preparation of Acidified $NaNO_2$

Stock solution of 100 mM acidified $NaNO_2$ was prepared by mixing dissolved sodium nitrite (in H_2O) with concentrated HCl in a 1:1 ratio (V/V). Final concentration of this mixture was used as the nitrosative stress reagent at requisite amount to have effective concentration of 0.5 mM, 1 mM, and 3 mM acidified $NaNO_2$. pH value after addition of such mixture to the media was also checked and found to be between 6.8 to 7.0, which is in the optimal range for *Saccharomyces cerevisiae* Y190 growth.

Cell Viability Assay

Yeast cells were grown in YPD medium treated with different concentration of acidified $NaNO_2$ (0 mM, 0.5 mM, 1 mM, and 3 mM) and incubated in shaking condition. After overnight incubation, 1 ml of culture from each sample from both media were serially diluted and plated on YPD agar medium for viable cell count. Under same condition, growth curve of samples were assessed to spectrophotometrically at 600 nm.

Detection of ROS and RNS

Presence of ROS and RNS were detected as per the protocol of Invitrogen with slight modifications. In short, 2×10^6 cells were resuspended in PBS buffer pH 7.4 and fixed by absolute ethanol. After that dyes were added

(H_2DCFDA for ROS and DAM-FM for RNS) at the final concentration of 1 µM and incubated for 30 min in dark. For fluorescent microscopy (optika) excitation was fixed at 495 nm and emission at 515 nm. Micrographs (40 ×) were repeated for at least three independent experiments.

Estimation of Ethanol Production

Ethanol was estimated both by spectrophotometer and HPLC. Spectrophotometrically, ethanol estimation was done, using modified potassium dichromate method [18]. In short, overnight incubated treated and untreated yeast cells were centrifuged. One milliliter supernatants from each sample were added in the mixture of 0.25 M potassium dichromate ($K_2Cr_2O_7$), 0.1 M silver nitrate ($AgNO_3$), and 6 N sulfuric acid (H_2SO_4). After incubation samples were diluted and O.D. was recorded at 560 nm. Presence of ethanol was checked by HPLC model accordingly Zuley et al. [19] using Hi-Plex Hcolumn with the flow rate of 1 ml/min.

Preparation of Cell Free Extract (CFE)

Overnight grown treated and untreated cultures were taken and centrifuged under cold condition. Supernatants were discarded and pellets were suspended in lysis buffer [100 mM Tris-HCl at pH 7.6, 150 mM NaCl, 1 mM SDS, 1 mM DTT, 2 mM EDTA, protease inhibitor cocktail (Sigma-Aldrich, St. Louis, MO, USA), 1 mM PMSF] and were lysed using glass beads and vortexed until lysis. The soluble fractions were collected by centrifugation and the concentration of protein was determined via Bradford assay [20].

Alcohol Dehydrogenase Assay

Activity of alcohol dehydrogenase was determined as the protocol of Sigma. In short, cell lysate was taken for the alcohol dehydrogenase assay. Reaction mixture contains 50 mM sodium phosphate buffer at pH 8.8, 95% V/V ethanol and 50 mM β-NAD as the final concentration and diluted cell free extract. Time scan was performed for 6 min at 340 nm. Spectrophotometrically, the difference in initial and final O.D. was recorded.

Alcohol Dehydrogenase Inhibition Assay

Yeast cells were grown in YPD medium treated with acidified 0.5 mM $NaNO_2$ after 3 h of inoculation. At the same time 0.1 mM 2,2,2-trifluoroethanol was added in the sample and incubated. Ethanol production was estimated at 560 nm to check the inhibition of alcohol dehydrogenase. Untreated yeast cells were taken as the control [21].

Ethanol Production by Immobilization of Nitrated Yeast Cell

For the immobilization assay *S.cerevisiae* cells were first grown overnight in specified media in the presence of 0.5 mM sodium nitrite. Next, the culture was centrifuged and the cell pellet was resuspended in PBS buffer pH 7.0. 1 ml of such resuspended cell was then added slowly with 1% sodium alginate. After that cells were transferred to 0.5 M $CaCl_2$ solution drop wise with the help of a syringe with the formation of Ca-alginate beads having immobilized yeast cells. For, ethanol production 20 such beads was used to inoculate a broth media. Ethanol concentration was determined as stated earlier [22].

Optimization of Ethanol Production by Central Composite Rotatable Design based (CCRD) Response Surface Methodology (RSM)

Optimization of ethanol production was carried out using central composite rotatable design based (CCRD) response surface methodology (RSM) in order to study the interaction effect between three independent variables viz., molasses concentration (C-source) (A), ammonium sulfate concentration (N-source) (B) and Incubation time of yeast (C) in the fermentation broth. Due to the presence of "axial points" around the centre point in the CCRD design curvature of the model is allowed. As suggested by Sahu et al. [23]. Three independent variables molasses concentration (A), ammonium sulfate concentration (B) and Incubation time of yeast (C) were used in five different coded levels ($-\alpha$, -1,0, $+1$, $+\alpha$). Table 1 represent the relationship between the coded level and actual values of each variables used in this study to optimize ethanol production.

The relation between the coded level of variables and actual values of the variables are explained by the following equation (Eq. 1):

$$X_a = (Z_a - Z_0)/\Delta Z \tag{1}$$

where, Xa is the coded value, Za is the actual value, Zo is the actual value at the centre point, and ΔZ is the step

Table 1 Coded and actual levels of variables used to construct the model

Factor	Unit	Coded Levels				
		$-\alpha$	-1	0	$+1$	$+\alpha$
A (Carbon source)	% W/V	0	5	12.50	20	25.11
B (Nitrogen source)	% W/V	0	0.05	1.02	2	2.66
C (Incubation time)	Hours	0	6	15	24	30.14

change of the variables. Total 20 experimental runs were conducted and the ethanol produced by the yeast was analyzed by the second order polynomial regression equation (2).

$$Y = a_0 + a_1x_1 + a_2x_2 + a_3x_3 + a_{11}x_1^2 + a_{22}x_2^2 + a_{33}x_3^2 + a_{12}x_1x_2 + a_{13}x_1x_3 + a_{23}x_2x_3 \quad (2)$$

where Y is the predicted ethanol production (g/l), a_0 is the intercept, X_i is the independent variables and a_i is the model coefficient parameters.

Statistical Analysis

All experiments were done in triplicate. Level of significance (p) was set at 0.05 for all experiments.

Results and Discussion

Effect on Cell Viability in the Presence of $NaNO_2$

Acidified sodium nitrite was used as a nitrosative stress agent in all our experiment to determine the sub-toxic dose of sodium nitrite, cellular viability was checked. After overnight stress in medium, it was observed that cellular viability was not significantly affected at 0.5 mM concentration of sodium nitrite (Fig. 1) as compared with the control set. Whereas in the presence of 1 mM and 3 mM sodium nitrite under the same experimental condition, cellular viability was seen to have decreased significantly. Growth curve experiment above same condition as above has also shown similar results with 0.5 mM concentration of sodium nitrite showing least effect as compared with 1 and 3 mM sodium nitrite (Fig. 2). Hence, the concentration of sodium nitrite was fixed to be at 0.5 mM for all our further experiments.

Effect of $NaNO_2$ on ROS and RNS Generation

Generation of ROS and RNS are important markers to study the redox homeostasis [24]. Thus, in this context, it was important to investigate the presence of the both ROS and RNS under our experimental condition. In both control and 0.5 mM acidified $NaNO_2$ treated yeast cells the generation of ROS and RNS were determined by fluorescent microscopy. Our result showed a significant change in RNS production in 0.5 mM acidified $NaNO_2$ treated yeast cells as compared with control set (Fig. 3). Whereas, we did not found any significant change in ROS generation in 0.5 mM acidified $NaNO_2$ treated yeast cells compared with control set (Fig. 4).

This result is very interesting in terms of our work. There was also no significant difference in the generation of ROS between both control and 0.5 mM acidified $NaNO_2$ treated yeast cells which indicates the presence of endogenous ROS in both control and treated yeast cells and 0.5 mM acidified $NaNO_2$ had no role in generation of ROS. Whereas, it is evident that 0.5 mM acidified $NaNO_2$ was responsible for

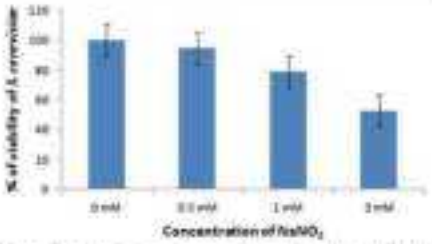

Fig. 1 Cell viability assay of untreated and treated (0.5, 1, 3 mM sodium nitrite) *S. cerevisiae*

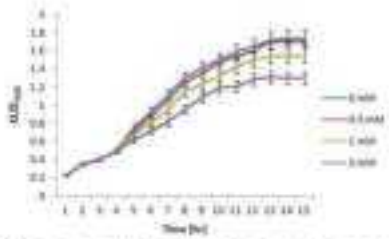

Fig. 2 Growth curve analysis: effect of nitrosative stress in untreated and treated (0.5, 1, 3 mM sodium nitrite) *S. cerevisiae*

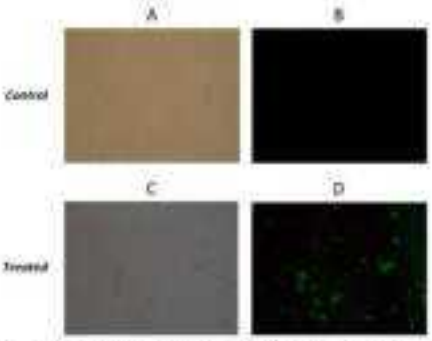

Fig. 3 Detection of RNS: the presence of RNS was visualized as green color. Fluorescence and corresponding phase contrast images of *S. cerevisiae* Y190 **a** and **b**. Control or untreated **c** and **d**. treated with 0.5 mM sodium nitrite

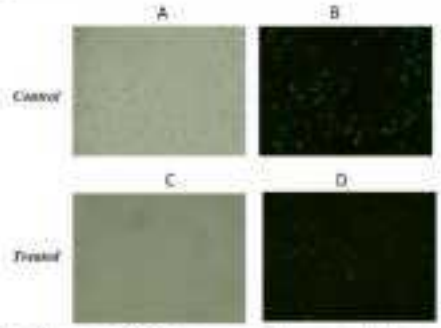

Fig. 4 Detection of ROS: the presence of ROS was visualized as green color. Fluorescence and corresponding phase contrast images of *S. cerevisiae* Y190 (a) and (b). Control or untreated (c) and (d) treated with 0.5 mM sodium nitrite

the generation of RNS. Thus, it can be concluded that the effect observed under our experimental condition was may be solely due to generation of RNS by of the 0.5 mM acidified $NaNO_2$.

Effect of $NaNO_2$ on Alcohol Production

As reported earlier, *S.cerevisiae* usually produces ethanol under aerobic condition [17], but this is much less as compared with fermentative condition. Under our experimental condition as mentioned in the materials and methods section ethanol production was found to be higher in the presence of 0.5 mM sodium nitrite stress as compared with the control. Our result suggests that in YPD medium ethanol production increased by 35% under nitrosative stress as compared with the control (Table 2). The result showed that under nitrosative stress the cellular metabolism flux and energy production has shifted significantly towards ethanol production, a major fermentative product. This may have happened due to alteration in biochemical pathways within the cell including modification of several important enzymes involved in cellular respiration and TCA cycle under nitrosative stress [10]. The presence of ethanol was also verified by HPLC (data not shown).

Effect of $NaNO_2$ on Alcohol Dehydrogenase Activity

In YPD medium, specific activity of alcohol dehydrogenase was significantly increased 34% when cells were treated with 0.5 mM $NaNO_2$ in comparison as compared with control (Table 3). To check that whether this alcohol production was solely due to the activity of ADH, an inhibitor assay was also performed. Addition of 2,2,2-trifluoroethanol as a competitive inhibitor of ADH, ceased the

Table 3 Ethanol production by treated and untreated *S. cerevisiae*

Sample	Ethanol (g/lit)
Control	21 ± 1
0.5 mM	28 ± 2

activity resulting in complete inhibition of alcohol production. Both the control and the treated sample have shown similar results (Table 3).

High amount of alcohol production in 0.5 mM $NaNO_2$ treated cells was due to the higher specific activity of alcohol dehydrogenase. Several studies reported that, aconitase, isocitrate dehydrogenase involved in TCA cycle can be nitrated in presence of NO or RNS resulting in inactivation of these enzymes [14]. So for the cell to survive, energy production via alteration biochemical pathways becomes essential. Therefore it is possible that, may be the cell was trying to reroute its metabolic flux toward fermentation. Alcohol dehydrogenase III, a mitochondrial protein is reported to be over expressed in nitrosative stress [25]. Glutathione dependent alcohol dehydrogenase also acts as a stress response enzyme, relieving the cell from nitrosative [25–28]. Altogether higher specific activity of ADH under experimental condition corroborates with the previous results and also suggests that it plays a vital role in energy production as well as stress reliever for a cell. This result clearly indicates that, alcohol dehydrogenase is the main enzyme responsible for the alcohol production at both stressed and unstressed condition in *Saccharomyces cerevisiae* [21].

Optimization of Ethanol Production by CCRD based RSM Technique

The effect of three independent variables molasses concentration (A), ammonium sulfate concentration (B), and incubation time (C) were tested for ethanol production by the yeast using CCRD based RSM technique. The optimal level for the each factor was determined. For optimization of ethanol production 19 experimental runs were performed and the results are represented in Table 4 with both the actual and model predicted responses.

Analysis of variance (ANOVA) was conducted for the above experimental design. The results are represented in Table 5. The results showed that the model is highly significant ($p < 0.003$) and can better predict the actual response i.e., ethanol production. Within the model molasses concentration (A) [$p = 0.0094$], incubation time (C) [$p = 0.0043$], molasses concentration^2 (A^2) [$p = 0.0030$] and incubation time^2 (C^2) [$p = 0.0045$] were the significant model terms. Using the result of this experimental design second-order polynomial regression equation is generated by software for ethanol concentration which is represented

Table 3 Specific activity of Alcohol Dehydrogenase of treated and untreated *S. cerevisiae*

SAMPLE	Specific activity of Alcohol Dehydrogenase (nM/min/mg)	Specific activity of Alcohol Dehydrogenase in the presence of 2,2,2-trifluoroethanol (nM/min/mg)
Control	10 ± 0.3	Not detected
0.3 mM	25 ± 0.4	Not detected

Table 4 Experimental design along with model predicted and actual ethanol yield response

Run	Factor 1A: C-source (%)	Factor 2B: N-source (%)	Factor 3C: Incubation (h)	Ethanol (g/l): Actual	Ethanol (g/l): Predicted
1	12.50	1.02	15.00	21.73	21.66
2	5.00	0.05	24.00	7.24	8.79
3	20.00	2.00	6.00	20.26	17.22
4	20.00	2.00	24.00	34.74	34.24
5	12.50	1.02	30.14	28.24	25.11
6	20.00	0.05	6.00	11.52	11.36
7	12.50	2.66	15.00	14.02	18.27
8	5.00	2.00	24.00	11.52	10.19
9	5.00	2.00	30.14	8.68	4.03
10	25.11	1.02	6.00	27.50	23.79
11	12.50	1.02	15.00	21.70	21.66
12	5.00	0.05	6.00	3.15	2.17
13	−0.11	1.02	15.00	0	5.23
14	12.50	1.02	15.00	21.69	21.66
15	12.50	1.02	15.00	21.75	21.66
16	12.50	1.02	−0.14	0	1.80
17	12.50	1.02	15.00	21.75	21.66
18	20.00	0.05	24.00	23.34	26.51
19	12.50	−0.61	15.00	12.35	10.20

in actual terms (Eq.3).

$$\text{R1(Ethanol concentration)}.\ \text{Actual} = -10.30525 + 1.38894 \times A + 5.61195 \times B + 1.03751 \times C + 0.17658 \times AB + 0.035870 \times AC + 0.020085 \times BC - 0.043112 \times A^2 - 2.76112 \times B^2 - 0.028324 \times C^2 \quad (3)$$

The R^2 value (coefficient of determination) of 0.9577 indicates that the model could explain the 93% variability in the model response. The predicted and adjusted R^2 0.5256 and 0.8817, respectively, were in reasonable agreement with each other. The model high adequate precision ratio of 13.864 indicates that high signal to noise ratio. Generally adequate precision ratio of 4 is desirable to judge the significance level of the model. In overall sense the R^2, adjusted R^2, predicted R^2, and adequate precision all are significantly higher and thus the model could be employed for identification of optimized level of each of the variables used for ethanol response.

Table 5 CCRD based RSM model

Source	Sum of squares	df	Mean square	F value	p value Prob > F
Model	890.41	9	98.93	7.52	0.0030
A: C-source	142.10	1	142.10	10.80	0.0094
B: N-source	9.99	1	9.99	0.76	0.4061
C: Incubation time	188.79	1	188.79	14.35	0.0043
AB	4.44	1	4.44	0.34	0.5756
AC	26.35	1	26.35	2.00	0.1907
BC	51.01	1	51.01	3.88	0.0819
A2	299.72	1	299.72	22.78	0.0010
B2	113.57	1	113.57	8.63	0.0165
C2	180.27	1	180.27	13.70	0.0045

Comparison of model actual and predicted values for ethanol response (g/l) is presented in Fig. 5. The plot showed that the observed and actual values were spited by a line of angle of 45°, indicating a reasonable agreement of predicted response with the actual ones.

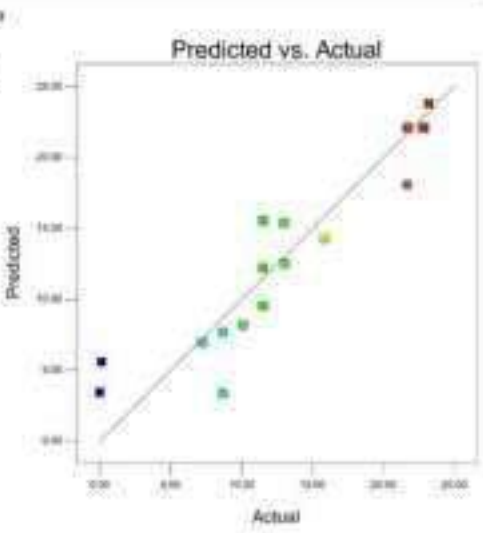

Fig. 5 Plot of actual values versus predicted values

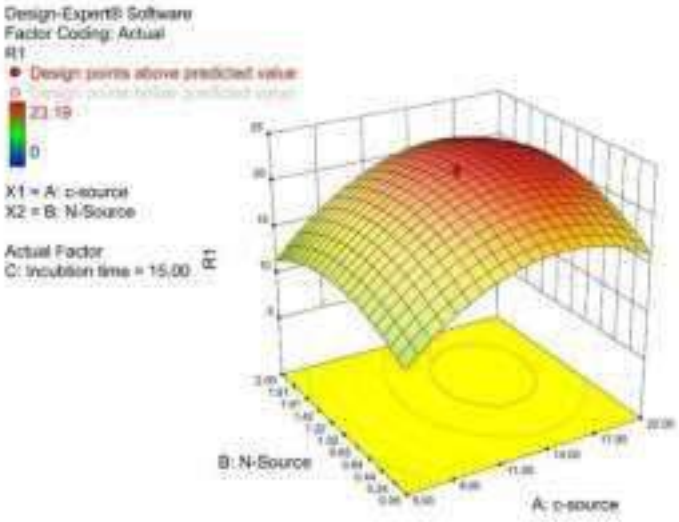

Fig. 6 Surface plot showing the effect of interaction between carbon source (Molasses) and nitrogen source (Ammonium sulfate)

The response surface plots and their contour plots described by second-order polynomial regression equation were generated in order to determine the interactions among variables and optimal level of variables for ethanol production (Figs. 6–8). It can be observed that the ethanol production was significantly varies with the molasses concentration (A) (Fig. 6). When the carbon source was enhanced from 5 to 20% W/V, keeping the nitrogen source fixed at 1.22% W/V, ethanol production was significantly enhanced from 11.88 to 27.54 g/l. The significance of the

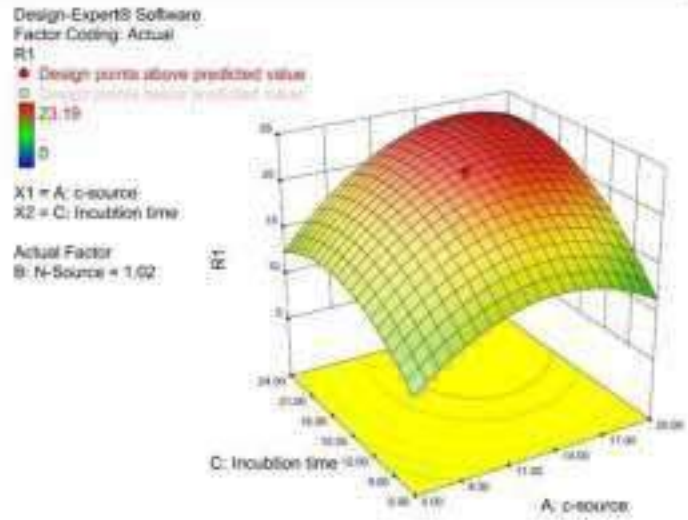

Fig. 7 Surface plot showing the effect of interaction between carbon source (Molasses) and incubation time

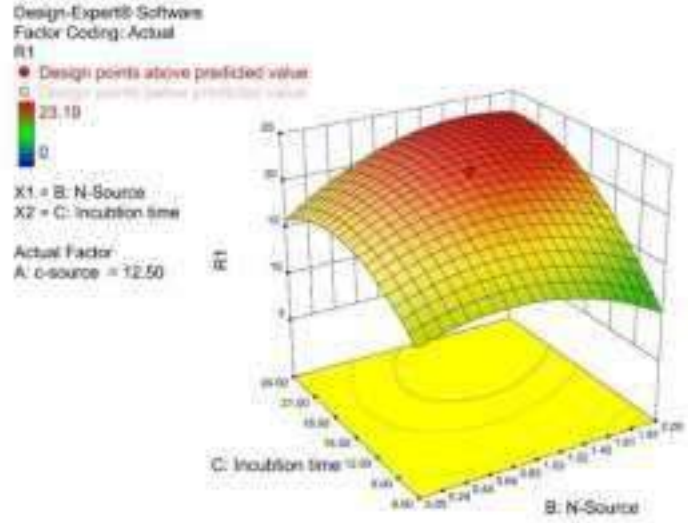

Fig. 8 Surface plot showing the effect of interaction between nitrogen source (Ammonium sulfate) and incubation time

carbon source was also confirmed from the ANOVA result which showed a p value of 0.0094.

The effect of interaction between the molasses concentration (A) and incubation time (C) is represented in Fig. 7 The result showed that along with carbon source, incubation time also significantly affect the ethanol production at a p value of 0.0043. Keeping the carbon source fixed at 20% W/V, when incubation time was gradually increased from 6 to 24 h, predicted ethanol production is also significantly enhanced from 16.37 to 32.90 g/l.

The effect of interaction between ammonium sulfate (B) and incubation time (C) is presented in Fig. 8 and it can be

Table 6 Ethanol production by immobilized yeast cells grown in YPD medium

	Immobilization		
No. of cycle	1st	2nd	3rd
Ethanol production (g/l)	33 ± 1	35 ± 2	27 ± 1

Table 7 Ethanol production by immobilized yeast cells grown in YPG medium

	Immobilization					
No. of cycle	1st	2nd	3rd	4th	5th	6th
Ethanol production (g/l)	31 ± 1	36 ± 2	39 ± 1	35 ± 1	24 ± 1	19 ± 1

observed from the plot that the ethanol production was not so much altered when either of the variables were increased or decreased. This result suggests, a non significant interaction between these two variables for ethanol production. This result is also supported by the ANOVA result where a p value of 0.0805 was obtained for these two variables. A mild increment of ethanol production was recorded from 20.24 to 25.18 g/l when nitrogen source concentration was increased from 0.05 to 2.00% W/V.

After careful analysis of the interaction between the variables for ethanol production, finally the model was employed to find out the optimized design space using the numerical optimization tool, where the response was asked for maximum level. It was obtained that carbon source concentration of 20.00% W/V, nitrogen source concentration of 1.74% W/V when used in the medium for 24 h of incubation time by the yeast, it will show 35.24 g/l of ethanol production which was very close to the model predicted response of 34.24 g/l.

Estimation of Ethanol Production by Yeast Cells under Nitrosative Stress Grown in YPG Medium

To assess the ability of nitrated yeast cells to produce ethanol over time, YPD grown stress exposed yeast cells were first immobilized in calcium alginate beads. The beads were then inoculated in fresh molasses containing medium to check for the production of ethanol. The process was repeated for several cycles using fresh molasses medium. Under our experimental condition it was observed that ethanol production with YPD grown stressed cells remains significantly unchanged for two cycles (Table 6). Whereas interestingly when YPG grown stressed yeast cells were used to repeat the same experiment, it was observed that ethanol production increased significantly upto 3rd cycles (Table 7). This may be due to the production of higher ROS and subsequently higher RNS by the yeast during their growth in respiratory proficient YPG media.

As ADH has a role in relieving the nitrosative stress [25], so with higher RNS accumulation, the expression of ADH might have significantly increased which eventually resulted in higher ethanol production. The gradual decrease in ethanol production with YPD and YPG grown immobilized yeast cells was may be due to cell death or changes in cellular physiology to relieve the effect of stress.

Conclusion

Under our experimental condition the present study showed that ethanol production by *Saccharomyces cerevisiae* increased, with the increase in ADH specific activity, when the cells were challenged with nitrosative stress. With the view to apply the process for industrial use, inexpensive nutrient sources were used during optimization. Moreover immobilization of yeast cells and its reuse for several cycles also helped in higher alcohol production and reduction of time and cost. This is the first report of this kind where an alternative method of ethanol production is explained with nitrated yeast cells. This approach is cost effective and productive. Therefore it holds a great promise for industrial production of fermented beverages, like beer, wine as well as bioethanol.

Acknowledgements The authors acknowledge the University of North Bengal for providing essential infrastructure and financial support to carry out this research.

Compliance with Ethical Standards

Conflict of Interest The authors declare that they have no conflict of interest.

References

1. Willaert, R. G. (2017). Yeast biotechnology. *Fermentation*, *3*, 7–10.
2. Mohd Azhar, S. H., Abdulla, R., & Jambo, S. A. et al. (2017). Yeasts in sustainable bioethanol production: a review. *Biochemistry and Biophysics Reports*, *10*, 52–61.
3. Verbelen, P. J., De Schutter, D. P., & Delvaux, F. et al. (2006). Immobilized yeast cell systems for continuous fermentation applications. *Biotechnology Letters*, *28*, 1515–1525.
4. Zaldivar, J., Nielsen, J., & Olsson, L. (2001). Fuel ethanol production from lignocellulose: a challenge for metabolic engineering and process integration. *Applied Microbiology and Biotechnology*, *56*, 17–34.
5. Nevoigt, E. (2008). Progress in metabolic engineering of *Saccharomyces cerevisiae*. *Microbiology and Molecular Biology Reviews*, *72*, 379–412.
6. Mitalbina, E., & Aranda, A. (2017). Biotechnological impact of stress response on wine yeast. *Letters in Applied Microbiology*, *64*, 103–110.

7. Pretorius, I. S. (2000). Tailoring wine yeast for the new millennium: novel approaches to the ancient art of winemaking. *Yeast, 16*, 675–729.
8. Forman, H., Fukuto, J. M., & Miller, T. (2008). The chemistry of cell signaling by reactive oxygen and nitrogen species and 4-hydroxynonenal. *Archives of Biochemistry and Biophysics, 477*, 183–195.
9. Palmer, R. M., Rees, D. D., & Ashton, D. S. (1988). L-arginine is the physiological precursor for the formation of nitric oxide in endothelium-dependent relaxation. *Biochemical and Biophysical Research Communications, 153*, 1251–1256.
10. Kurutas, E. B. (2016). The importance of antioxidants which play the role in cellular response against oxidative/nitrosative stress: current state. *Nutrition Journal, 15*, 71. https://doi.org/10.1186/s12937-016-0186-5.
11. Bhattacharjee, A., Majumdar, U., & Maity, D. et al. (2010). Characterizing the effect of nitrosative stress in *Saccharomyces cerevisiae*. *Archives of Biochemistry and Biophysics, 496*, 109–116.
12. Rogstam, A., Larsson, J. T., & Kjelgaard, P. (2007). Mechanisms of adaptation to nitrosative stress in *Bacillus subtilis*. *Journal of Bacteriology, 189*, 3063–3071.
13. Fang, F. C. (2004). Antimicrobial reactive oxygen and nitrogen species: concepts and controversies. *Nature Reviews Microbiology, 2*, 820–832.
14. Bhattacharjee, A., Majumdar, U., & Maity, D. et al. (2009). In vivo protein tyrosine nitration in *S. cerevisiae*: Identification of tyrosine-nitrated proteins in mitochondria. *Biochemical and Biophysical Research Communications, 388*, 612–617.
15. Crow, J. P., Beckman, J. S., & McCord, J. M. (1995). Sensitivity of the essential zinc-thiolate moiety of yeast alcohol dehydrogenase to hypochlorite and peroxynitrite. *Biochemistry, 34*, 3544–3552.
16. Claudia, L., Natalya, L., & Müller, A. (2013). Redox proteomics uncovers peroxynitrite-sensitive proteins that help *Escherichia coli* to overcome nitrosative stress. *The Journal of Biological Chemistry, 288*, 19608–19714.
17. Hagman, A., Sall, T., & Compagno, C., et al. (2013). Yeast 'make-accumulate-consume' life strategy evolved as a multi-step process that predates the whole-genome duplication. *PLoS ONE, 8*, e68734.
18. Sayyad, S. F., Chaudhari, S. R., & Panda, B. P. (2015). Quantitative determination of ethanol in solids by using UV-visible spectrophotometer. *Pharmaceutical and Biological Evaluations, 2*, 204–207.
19. Zakya, A. S., Pennapa, N., & Andrade-Eiroa, Á. (2017). A new HPLC method for simultaneously measuring chloride, sugars, organic acids and alcohols in food samples. *Journal of Food Composition and Analysis, 56*, 25–33.
20. Bradford, M. M. (1976). A rapid and sensitive method for the quantitation of microgram quantities of protein utilizing the principle of protein-dye binding. *Analytical Biochemistry, 72*, 248–254.
21. Bichsel, L. T. (1998). The competitive inhibition of yeast alcohol dehydrogenase by 2,2,2-trifluoroethanol. *Biochemical Education, 26*, 239–242.
22. Pereira, A. P., Estevinho, L. M., & Mendes-Faia, A. (2014). Mead production: fermentative performance of yeasts entrapped in different concentrations of alginate. *Journal of the Institute Brewing, 120*, 575–580.
23. Saha, S. P., & Ghosh, S. (2014). Optimization of xylanase production by *Penicillium citrinum* xyn2 and application in saccharification of agro-residues. *Biocatalysis and Agricultural Biotechnology, 3*, 188–196.
24. Dhawan, V. (2014). Reactive oxygen and nitrogen species: general considerations. In N. K. Ganguly, S. K. Jindal, S. Biswal, P. J. Barnes & R. Pawankar Eds., *Studies on Respiratory Disorders* (pp. 27–47). New York, NY: Humana Press.
25. Staab, C. A., Ahnlund, J., & Brandt, M. (2008). Reduction of S-nitrosoglutathione by alcohol dehydrogenase III is facilitated by substrate alcohols via direct cofactor recycling and leads to GSH-controlled formation of glutathione transferase inhibitors. *Biochemical Journal, 413*, 493–504.
26. Gow, A. J., & Stamler, J. S. (1998). Reaction between nitric oxide and haemoglobin under physiological conditions. *Nature, 391*, 169–173.
27. Sahoo, R., Bhattacharjee, A., & Majumder, U. et al. (2009). A novel role of catalase in detoxification peroxynitrite in *Saccharomyces cerevisiae*. *Biochemical and Biophysical Research Communications, 38*, 5507–5511.
28. Liu, L., Hausladen, A., & Zeng, M., et al. (2001). A metabolic enzyme for S-nitrosothiol conserved from bacteria to humans. *Nature, 410*, 490–494.

Process Biochemistry 113 (2022) 62–70

Contents lists available at ScienceDirect

Process Biochemistry

journal homepage: www.elsevier.com/locate/procbio

Short communication

Characterizing the effect of *S*-nitrosoglutathione on *Saccharomyces cerevisiae*: Upregulation of alcohol dehydrogenase and inactivation of aconitase

Swarnab Sengupta, Rohan Nath, Arindam Bhattacharjee *

Department of Microbiology, University of North Bengal, India

ARTICLE INFO

Keywords:
Saccharomyces cerevisiae
Aconitase
Nitrosative stress
GSNO
adh3

ABSTRACT

When exposed to nitrosative stress, the redox status of *Saccharomyces cerevisiae* changes significantly in vivo. Under nitrosative stress, aconitase, which catalyzes the conversion of citrate to isocitrate in the tricarboxylic acid (TCA) cycle, is known to be vulnerable. In this study, aconitase was completely repressed in the presence of 0.25 mM *S*-nitrosoglutathione (GSNO) as the nitrosative stress agent. Furthermore, a ~1.5 fold increase in ethanol production and a 3.5 fold increase in alcohol dehydrogenase (ADH) activity were observed in the presence of 0.25 mM GSNO when compared to the control (untreated). Furthermore, we supported our findings with a gene expression study of the *adh3* gene, which showed a 4 fold increase in the presence of 0.25 mM GSNO. This is the first report of its kind to characterize ethanol production under GSNO stress. This study may prove to be industrially significant in ethanol production.

1. Introduction

GSNO is a well-known endogenous •NO donor that can play a significant role in the alteration of redox homeostasis *in vivo* [1]. A large body of research in stress biology indicates that GSNO can be used as a nitrosative stress agent [2–7]. Reactive nitrogen species (RNS), which form inside the cell during nitrosative stress, have the ability to modify biomolecules such as DNA and proteins [1–5]. The change in redox homeostasis *in vivo*, which may lead to changes in the physicochemical properties of the cell, is one of the most significant hallmarks of nitrosative stress [8]. RNS includes nitric oxide radicals (•NO), peroxynitrite ($ONOO^-$), and nitrogen oxide radicals(NO_2^-). These are formed when reactive oxygen species (ROS) react with nitric oxide [10]. Nitric oxide is a freely diffusible, short-lived, lipophilic molecule. At low concentration, •NO is involved in cell signaling, but at high concentrations, it binds to heme, iron, and copper-containing proteins [11–13] and becomes toxic to the cell. •NO and RNS both exhibit cytotoxic and cytostatic activities due to the inhibition of ATP production, altered iron metabolism, enzyme inhibition, DNA and DNA repair system damage [5, 11,14–20]. To counteract the hostile condition, various stress response enzymes such as catalase, glutathione reductase (GR), SOD, and others are activated [6,21,22].

S. cerevisiae is an excellent model for studying the effects of nitrosative stress. It has been reported that GSNO stress affects aconitase (aconitate hydratase, EC 4.2.1.3), an important enzyme of the TCA cycle in *S. cerevisiae* [2,23]. As a result, inhibiting aconitase activity may have an effect on the aerobic respiration of *S. cerevisiae*. Alcohol dehydrogenase (ADH3) has been reported to act as a stress-response enzyme during nitrosative stress using GSNO [24,25]. Thus, using GSNO under nitrosative stress may cause a change in cellular metabolism, which may eventually lead to increased ethanol production via the fermentative pathway. However, no such report exists that characterizes the effect of GSNO on ethanol production by *S. cerevisiae*. Although many studies on metabolic engineering in *S. cerevisiae* have been conducted [26–30], certain drawbacks such as complexity, mutation, human safety, costing, and time consumption remain [29–32]. Furthermore, such procedures are prohibitively expensive [29–33]. Thus, one of the major areas of interest is an alternative, cost-effective, and simple process for increasing ethanol production by *S. cerevisiae*.

As a result, the objectives of this study were to examine the effect of

Abbreviations: S. cerevisiae, *Saccharomyces cerevisiae*; SOD, super oxide dismutase; $HClO_4$, perchloric acid; KOH, potassium hydroxide; DTNB, 5,50-dithio-bis (2-nitrobenzoic acid); PBS, phosphate Buffer Solution; TCA, trichloroacetic acid; CTAB, hexadecyltrimethylammoniumbromide; $KMnO_4$, potassium permanganate; DNS, 3, 5-dinitrosalicylic acid; qPCR, Quantitative Real-time PCR; cDNA, complementary DNA; SD, standard deviation.

* Corresponding author at: Department of Microbiology, University of North Bengal, West Bengal, India.
E-mail address: arindambnu@gmail.com (A. Bhattacharjee).

https://doi.org/10.1016/j.procbio.2021.12.001
Received 9 February 2021; Received in revised form 4 December 2021; Accepted 10 December 2021
Available online 11 December 2021

nitrosative stress by GSNO on ethanol production by *S. cerevisiae* and to look for any changes in metabolic activity from respiration to fermentation. This is the first report of its kind that directly correlates ethanol production with a simple, cost-effective, and ecofriendly process involving nitrosative stress.

2. Materials and methods

2.1. Yeast culture and growth

Wild type haploid *S. cerevisiae* Y190 [ATCC 96400], a gift from Prof. Sanjay Ghosh CU, was used for all experiments. Cells were grown in YPD (2 % W\V yeast extract, 2 % W\V peptone, and 2 % W\V dextrose) medium at 30 °C under shaking condition (80 RPM). The single colonies containing YPD agar plates were kept at 4 °C refrigerator and 50 % glycerol stocks were kept at − 20 °C freezer. The glycerol stock was used for the preparation of preinoculum. 200 µl. from the glycerol stock was inoculated in a fresh YPD broth and incubated overnight at 30 °C. After that, streak plating was done on YPD agar plate using the overnight grown culture and incubated overnight at 30 °C to isolate single colonies. Following that, the culture was checked for contamination by phase contrast microscopy. Then pre-inoculum was prepared by inoculating single isolated colony in YPD broth and again incubated overnight at 30 °C. The overnight grown *S. cerevisiae* cells were then used as inoculum for further experiments.

2.2. Preparation of S-nitrosoglutathione

GSNO was prepared according to the method of Hart with slight modifications [34]. In short, 0.5 M GSNO was obtained by mixing 1 M of $NaNO_2$ (Sigma-Aldrich) in double-distilled water and 1 M GSH (Himedia) in 1 N HCl in cold (1:1 V/V). The concentration of GSNO was measured spectrophotometrically (ThermoScientific MultiskanGO) at 335 nm. The above mentioned instrument was used for all other spectrophotometric studies.

2.3. Cell viability assay

Mid-log phase yeast cells were grown in YPD medium treated with different concentrations of GSNO (0.25 mM, 0.5 mM, 1 mMmM) and incubated overnight in shaking condition. Following an overnight incubation, 1 ml of culture from each sample was serially diluted and plated on YPD agar medium for viable cell count. As a control, a culture with no GSNO was used. The growth curve was created by recording the O.D. at 600 nm for 11 h at 60 min intervals [35]. The growth curve was used to calculate the specific growth rate. Additionally, growth curve was also studied upto 48 h.

2.4. Preparation of cell-free extracts (CFE) and estimation of protein

Cell-free extract (CFE) of treated and untreated cultures were prepared for different enzymatic assays. Overnight grown cultures of treated and untreated samples were centrifuged, and the supernatants were discarded. The cell pellets were lysed by using glass beads and lysis buffer containing 100 mM Tris-HCl (pH 7.6), 150 mM NaCl, 1 mM SDS, 1 mM DTT, 2 mM EDTA, protease inhibitor cocktail (Sigma-Aldrich), and 1 mM PMSF [3]. The concentration of protein was estimated as per the Bradford protocol. The standard curve for estimation of protein concentration was prepared by using BSA [36].

3. Assay of redox homeostasis

3.1. Reduced to oxidized glutathione ratio

The concentrations of GSH (reduced glutathione) and GSSG (oxidized glutathione) were determined using the method described by Akerboom et al. [37]. CFEs (from both treated and untreated samples) were first deproteinized with 2 M $HClO_4$ (Merck), 2 M EDTA (Himedia), and then neutralized with 2 M KOH (Himedia), 0.3 M HEPES (Himedia) to pH 7. After centrifuging one portion of the neutralized samples at 5000 *g* for 5 min, the supernatants were collected to determine the total *in vivo* thiol concentration (GSH + GSSG) using Glutathione Reductase (GR) dependent DTNB (Himedia) reduction method. Another portion of the samples was treated with 2-vinylpyridine (50:1 V/V) for 60 min and used to determine GSSG. Time scan was done at 412 nm for 3 min. Both GSH and GSSG concentrations were expressed in nmol/mg of protein.

3.2. Glutathione reductase assay

The glutathione reductase assay was performed according to the protocol of Carlberg and Mannervik with slight modification [38]. In brief, 2 mM GSSG (Himedia), 3 mM DTNB, and 2 mM NADPH (Himedia) were mixed with an assay buffer containing 1 mM EDTA and CFE. Time scan was done at 412 nm for 3 min. Reaction mixture without CFE was taken as a baseline. Specific activity was expressed in mU/mg of protein.[1]

3.3. Catalase assay

Catalase activity was assayed according to the method of Aebi with slight modification [39]. In brief, H_2O_2 degradation was measured spectrophotometrically at 240 nm for 2 min. The reaction mixture contained 0.1 M potassium phosphate buffer at pH 7.5, 50 mM EDTA, H_2O_2 (Sigma-Aldrich), and CFE. Reaction mixture without CFE was taken as a baseline. Specific activity was expressed in mU/mg of protein[1].

3.4. S-nitrosoglutathione reductase (GSNOR) assay

GSNO Reductase assay was performed according to the protocol of Sahoo et al. with slight modifications [3]. In brief, 100 mM GSNO, 0.2 mM NADH (Himedia), and 0.5 mM EDTA were mixed in 20 mM Tris-Cl pH 8.0 with CFE. The conversion of NADH to NAD was recorded at 340 nm for 5 min. Reaction mixture without CFE was taken as a baseline. Specific activity was expressed in mU/mg of protein.

3.5. Confocal microscopy

Confocal microscopy (Leica TCS SP8) was used to detect nitric oxide (NO) and reactive oxygen species (ROS). NO and ROS were detected using the Invitrogen protocol, with some modifications. In brief, 2×10^6 cells were washed and resuspended in PBS pH 7.4 before being fixed with absolute ethanol. The dyes (H_2DCFDA [Invitrogen] specific for ROS and DAF-FM [Invitrogen] specific for NO) were then added at a final concentration of 1.5 µM and incubated in the dark for 20 min. Excitation was set to 495 nm for confocal microscopy and emission to 515 nm. The positive control for ROS analysis was prepared with 0.1 mM H_2O_2 treated *S. cerevisiae* cells. Experiments for NO and ROS were repeated independently at least three times and micrographs (45X) were taken. The intensity of fluorescence was quantified with at least 50 no. of cells for each sample assayed using the Leica LAS X software.

3.6. Aconitase assay

Aconitase assay was performed according to the protocol of Castro et al. [40] with slight modifications. In brief, the formation of isocitrate (Sigma-Aldrich) from cis-aconitate was determined

[1] mU/mg of protein is defined as 1 mg of protein that catalyzes the conversion of one nanomole of substrate per minute under the specified conditions of the assay method.

spectrophotometrically at 240 nm for 3 min. The reaction mixture contained 500 mM cis-aconitate, 100 mM Tris-Cl pH 8 with CFE. Reaction mixture without CFE was taken as a baseline. Specific activity was expressed in mU/mg of protein.

3.7. Estimation of ethanol and reducing sugar

Ethanol and reducing sugar concentrations were estimated as per the protocol of Zhang et al. with slight modifications [41]. In brief, overnight grown untreated and treated *S. cerevisiae* broth cultures were centrifuged at 5000 g, and supernatants were collected. After that supernatants were mixed with equal volume of 20 % TCA at room temperature for 5 min and then centrifuged at 10,000 g. The supernatants were then treated with 1/5 vol of 20 % CTAB at 65 °C for 10 min and again centrifuged at 10,000 g. These pretreated samples were then diluted 100 folds for ethanol estimation. Pretreated samples are mixed with $KMnO_4$ solution and incubated at 40 °C for 90 min. Initial and final O.D. were recorded at 526 nm. Standard curve for the ethanol estimation was prepared by using absolute ethanol (Merck). The 10-fold diluted pretreated sample was mixed with DNS solution for the estimation of sugar concentration. Standard curve for reducing sugar estimation was prepared by using glucose (Merck). Further, ethanol yield and productivity were determined as mentioned by Mithra et al. with slight modification [42].

3.8. Alcohol dehydrogenase assay

Alcohol dehydrogenase activity was determined as per the protocol of Walker with some modifications [43]. In brief, the reaction mixture contained 50 mM sodium phosphate buffer at pH 8.8, 95 % V/V acetaldehyde (Sigma-Aldrich), 50 mM β-NADH, and diluted CFE. The O.D. was recorded at 340 nm for 6 min to determine the formation of β-NAD from β-NADH. Reaction mixture without CFE was taken as a baseline. Specific activity was expressed in mU/mg of protein.

3.9. In vitro study of alcohol dehydrogenase

ADH was studied *in vitro* by directly adding GSNO to the CFE. Cells were first grown under the previously mentioned conditions, and CFE was prepared. The CFE was then treated directly with 0.25 mM GSNO for 60 min. Following that, the ADH activity of treated and untreated samples determined, as previously stated [43]. The experiment was repeated with pure ADH (Sigma-Aldrich).

4. Gene expression analysis of *adh1, adh2, adh3* by quantitative Real Time PCR

4.1. RNA isolation

RNA isolation was carried out in accordance with the protocol developed by Dr. KPC Life Sciences in India, using their developed kit containing columns. Overnight grown treated and untreated *S. cerevisiae* cultures were centrifuged at 5000g, and pellets were washed twice with 1X PBS. After adding buffers, the entire solution was transferred to the prelim column and centrifuged at 10,000 g. The column was discarded and isopropanol was added and transferred to a Chrome column and centrifuged at 10,000 g. The chrome column was then washed and centrifuged at 10,000 g for 10 min. Finally, RNA was eluted in 50 µl nuclease-free water and quantified using 1 % agarose TAE gel. For each set of experimental conditions, at least two biological replicates were used.

4.2. cDNA preparation

The template for cDNA synthesis was 500 ng of RNA from each sample. RNA was denatured at 65 °C for 5 min with 10 mM dNTP and 10 mM random hexamer. The mixture was then immediately chilled on ice. The reverse transcriptase (RT) enzyme (Thermo Scientific) was then mixed in 5X RT specific buffer and incubated at 42 °C for 60 min before being heat inactivated at 65 °C for 15 min.

Table 1
Primers used in this study.

Primers	Sequences (5′→3′)
adh1F	GTTGCCATCTCTGATTGCTTC
adh1R	ACACCATTGAGGGCCACCTTT
adh2F	GTTACACCCACCACGATTTCT
adh2R	ACGGTGGTACCCTTCAGCTCT
adh3F	CTGTCCTCACGCTGACTTGT
adh3R	CAACAATACCGTTTGGCCTA
gapdhF	GGGTAGATTGGTCATGAGAAT
gapdhR	TGGTACAAGAAGGTTTGAAAA

4.3. Quantitative real time PCR set up

Quantitative Real-time PCR (Biorad CFX-96) reaction was performed with SUPER2yn qPCR mastermix (Dr. KPC Life sciences) in the desired reaction conditions. One reaction (+RT) was setup using synthesized cDNA as the template for qPCR. The diluted RNA sample was used as the template in another reaction (-RT). This is done to ensure that the isolated RNA is free of DNA contamination. Another negative control (NTC) with no template was set up. This was a two-step PCR with denaturation at 95 °C for 15 s, annealing, and extension at 60 °C for 30 s. For qPCR, the number of cycles was 40, followed by a melt curve. All + RT reactions were carried out in triplicate. Table 1 contains a list of primers.

4.4. Statistical analysis

All individual results are expressed as mean ± SD (Standard deviation) of at least three independent experiments for each biological sample, where applicable. To analyze the significant difference between control and treated samples, Student *t*-test was used at 0.05 level of significance (p).

5. Results

5.1. Effect of S-nitrosoglutathione on cellular viability of S. cerevisiae

To determine the sub-toxic dose, cell viability of *S. cerevisiae* Y190 was tested in the presence of various concentrations of GSNO (0 mM, 0.25 mM, 0.5 mM, 1 mM). After an overnight incubation under shaking conditions, it was discovered that the presence of 0.25 mM GSNO in the medium had no effect on cell viability when compared to the control (0 mM GSNO). In the presence of 0.5 mM and 1 mM GSNO, under the same experimental conditions, cellular viability was significantly affected by nearly 30 % and 60 %, respectively, as compared to control **[Fig. S1]**. In comparison to the control, the growth curve of *S. cerevisiae* was found to be unaltered in presence of 0.25 mM GSNO **[Fig. S2]**. Furthermore, specific growth rate was also estimated from the growth curve, and no difference was found between control and treated *S. cerevisiae* ($0.22hr^{-1}$). As a result, the concentration of GSNO was set to 0.25 mM for all subsequent experiments.

5.2. Effect on redox homeostasis in the presence of S-nitrosoglutathione

To investigate the alteration in redox homeostasis *in vivo* under nitrosative stress, GSSG/GSH ratio, GR, GSNOR, and catalase activity, were assessed.

According to the results, the total content of oxidized glutathione (GSSG) was decreased by 2.4 fold and reduced glutathione (GSH) was increased by 1.6 fold in the 0.25 mM GSNO treated cells, resulting in a 3.9 fold increase in the GSH/GSSG ratio when compared to the control

Table 2
Estimation of total glutathione (GSH + (2GG), GSH/GSSG and activity of glutathione reductase (GR), Catalase and S-nitrosoglutathione reductase (GSNOR) in both treated and untreated (control) samples of *S. cerevisiae*.

Sample	(GSH + GSSG) nmol/mg of protein	GSH nmol/mg of protein	GSSG nmol/mg of protein	GSH/GSSG	GR Activity (nU)/mg protein)	Catalase Activity (nU)/ mg protein)	GSNOR Activity (nU)/ mg protein)
Control	92 ± 2	34 ± 0.5	46 ± NA	0.7	4 ± 0.3	4 ± 0.4	1 ± 0.02
0.25 mM GSNO	75 ± 2	55 ± 0.4	20 ± NA	2.75	14 ± 0.7	19 ± 0.5	4 ± 0.3

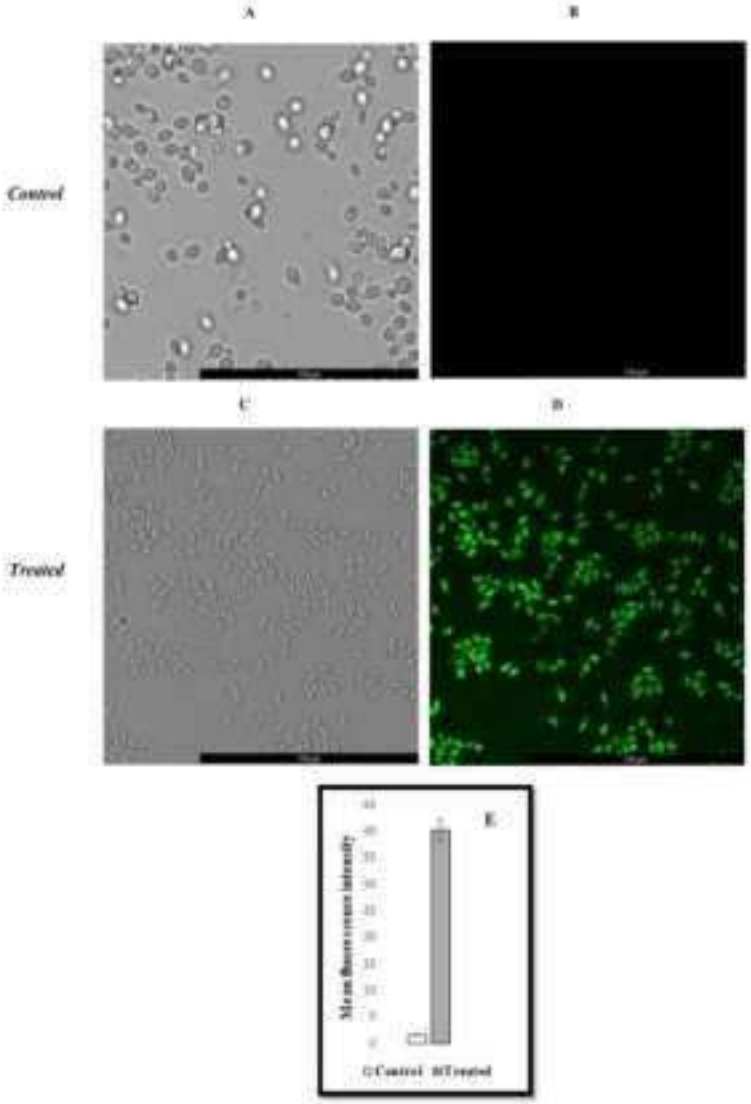

Fig. 1. Effect of S-nitrosoglutathione on nitric oxide (NO) generation: The presence of NO was visualized as green colour using DAF-FM (excitation at 495 nm and emission at 515 nm). Phase contrast and corresponding fluorescence images of *S. cerevisiae* control (A and B) and 0.25 mM GSNO treated (C and D). Micrographs were recorded at 45 ×. Bar = 100 μm. The mean fluorescent intensity (E) was determined by using Leica LAS X software and represented as mean ± SD.

[Table 2]. The enzyme GR is responsible for catalyzing the conversion of GSSG to GSH [3]. As a result, we tested the GR activity of both treated and untreated samples. We discovered a 3.36fold increase in GR activity in the treated cells [Table 2]. This result supports the previous finding about the GSH/GSSG ratio. Furthermore, treated cells also showed 4.3 fold higher activity of GSNOR (GSNO reductase) as compared to control,

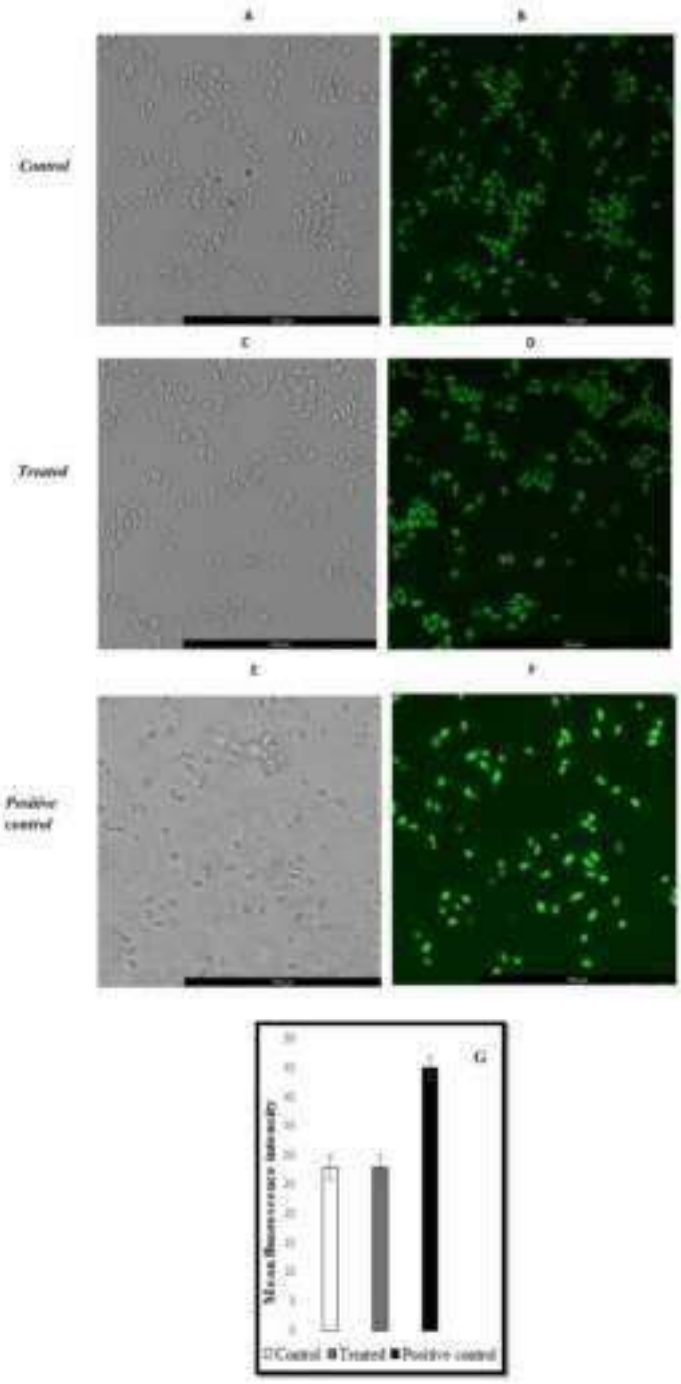

Fig. 2. Effect of S-nitrosoglutathione on reactive oxygen species (ROS) generation: The presence of ROS was visualized as green colour using H_2DCFDA (excitation at 495 nm and emission at 515 nm). Phase contrast and corresponding fluorescence images of *S. cerevisiae* control or untreated (A and B), 0.25 mM GSNO treated (C and D) and positive control [0.1 mM H_2O_2 treated] (E and F). Micrographs were recorded at 45 ×. Bar = 100 μm. The mean fluorescent intensity (G) was determined by using Leica LAS X software and represented as mean ± SD.

Table 3
Estimation of aconitase activity of treated and untreated (control) samples of *S. cerevisiae*.

Sample	Aconitase Activity (nU/mg protein)
Control	7 ± 0.21
0.25 mM GSNO	Not Detected

indicating that cells were expressing these enzymes to nullify the effect of GSNO [Table 3]. In the case of catalase, a general stress response enzyme, there was a 2.6 fold increase in specific activity in treated cells compared to controls [Table 2], implying that any ROS produced during the process was detoxified.

5.3. Effect of S-nitrosoglutathione on reactive oxygen species (ROS) and nitric oxide (NO) generation

To study redox homeostasis, it was critical to investigate the generation of ROS and NO [12]. The presence of ROS and NO was detected in our experimental conditions using confocal microscopy and mean fluorescence intensity. Surprisingly, NO was only detected in GSNO-treated cells [Fig. 1]. Untreated cells contained no NO. Whereas ROS was found in both the treated and untreated samples, there was no significant difference in ROS generation [Fig. 2]. As a result of the obtained data, it is possible to conclude that the effect observed under our experimental conditions is solely due to the generation of NO by 0.25 mM GSNO.

5.4. Effect of S-nitrosoglutathione on aconitase activity

It has previously been reported that nitrosative and oxidative stress can affect the activity of aconitase, a key enzyme in the TCA cycle [40, 44]. As a result, we used the aconitase assay in this study [Table 3]. Although aconitase activity was detected in untreated cells, it was not detected in cells treated with 0.25 mM GSNO. The result was particularly intriguing because it suggests that aconitase activity was suppressed under our experimental conditions.

5.5. Effect of S-nitrosoglutathione on ethanol production

When 0.25 mM GSNO was present, ethanol production increased significantly (~1.5 fold) when compared to the control [Table 4]. The ethanol yield was increased by approximately 1.3 fold and consumption of sugar was also 15 % higher under the stress condition. The volumetric productivity was also increased by approximately 1.5 fold in the presence of 0.25 mM GSNO. 76 % of the theoretical ethanol yield was found in the presence of 0.25 mM GSNO whereas only 59 % of the theoretical ethanol yield was found in untreated sample. Under our experimental conditions, these results suggest a possible shift in metabolic flux from respiration to fermentation.

5.6. Effect of S-nitrosoglutathione on alcohol dehydrogenase activity

Because ethanol production had increased, it was critical to investigate the activity of alcohol dehydrogenase. In this study, we discovered that ADH activity increased by 3.5 fold in the presence of 0.25 mM GSNO when compared to the control [Table 5]. Interestingly, no change in ADH activity was observed when an *in vitro* study was performed using CFE [Table 6], implying that GSNO may not be involved in ADH protein modification. ADH inhibition was also studied using 0.1 mM 2,2,2-trifluoroethanol. When the experiment was done with pure ADH, a similar type of result was obtained **[Fig. S3]**.

5.7. Effect of S-nitrosoglutathione on the expression of adh genes (adh1, adh2, adh3)

The expression levels of three important genes (*adh1*, *adh2*, *adh3*) were examined to determine the reason for the increased enzymatic activity of ADH in the presence of 0.25 mM GSNO. The expressions of *adh1* **[Table S1A]** and *adh2* **[Table S1B]** were found to be increased by only 7 % and 5 %, respectively, whereas *adh3* expression **[Table S1C]** was found to be increased by 4 fold in the presence of 0.25 mM GSNO compared to the control [Fig. 3]. This result suggested that increased ADH enzyme activity in the presence of 0.25 mM GSNO was primarily due to an increase in *adh3* expression.

6. Discussion

We have reported for the first time in this study the relationship between GSNO stress and ethanol production by *S. cerevisiae*. Under subtoxic dose of GSNO stress, we found some significant changes in physicochemical properties of *S. cerevisiae* compared to control, indicating that the cells were attempting to combat the stress for survival. A significant 4.3 fold increase in GSNOR specific activity, for example, suggests that *S. cerevisiae* cells were attempting to counteract the stress imposed by GSNO by upregulating an enzyme that can reduce it to form GSSG. Again, the higher activity of GR converted GSSG to GSH, implying that an elevated level of reduced equivalents is required to maintain redox homeostasis *in vivo*. GSH is regarded as a stress response component that protects cells from reactive species-mediated cellular damage, metal toxicity, and so on [21,45]. Intracellular GSH plays an important role in the inhibition of NO activity [45,46]. When the GSH level decreases, NO activity induces DNA damage as well as protein modifications such as protein tyrosine nitration, *S*-nitrosylation and so on [47, 48]. According to some reports, GSNO acts as a reservoir of NO that can be transported outside the cell *via* a GSH transporter system [45,49]. As a result, the GSH can also maintain the cellular redox balance *via* the elimination of the nitrating agent. Catalase, which is known for its

Table 5
Estimation of alcohol dehydrogenase activity of treated and untreated (control) cells of *S. cerevisiae*.

Sample	Alcohol dehydrogenase Activity (nU/mg protein)
Control	10 ± 0.2
0.25 mM GSNO	35 ± 0.5

Table 6
Estimation of alcohol dehydrogenase activity of treated and untreated cell free extract (CFE) and treated CFE.

Condition	ADH activity (nU/mg)
CFE	4 ± NA
0.25 mM GSNO treated CFE	4 ± NA
CFE + 2,2,2- trifluoroethanol	Not found
0.25 mM GSNO treated CFE + 2,2,2- trifluoroethanol	Not found

Table 4
Estimation of ethanol concentration, glucose consumption, ethanol yield, percentage of theoretical yield and volumetric productivity of treated and untreated (control) samples of *S. cerevisiae*.

Sample	Ethanol concentration (g/L)	Glucose consumed (g/L)	Ethanol yield (g/g of glucose)	% of theoretical yield	Volumetric Productivity (g/L/h)
Control	4.5 ± 0.3	15 ± 0.3	0.30	59	0.30
0.25 mM GSNO	7 ± 0.5	18 ± 0.4	0.39	76	0.56

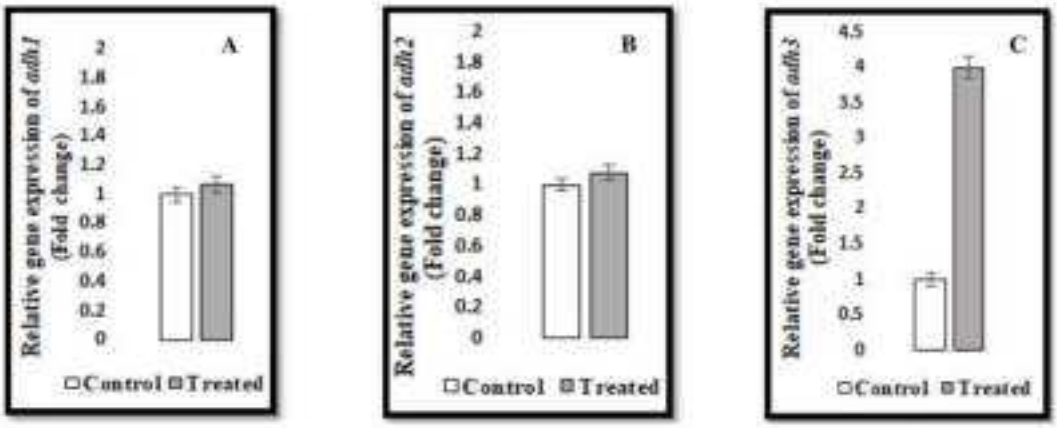

Fig. 3. Effect of S-nitrosoglutathione on adh genes expression: *qPCR analysis was done to determine the* **a.** *relative expression of adh1* **b.** *relative expression of adh2 and* **c.** *relative expression of adh3. The expression levels of adh genes (adh1, adh2 and adh3) were normalized with that of gapdh (glyceraldehyde-3-phosphate dehydrogenase) in each set and expressed as relative fold change taking the normalized expression level in respective untreated control as unity.*

catalytic detoxification of oxidants, was found to be upregulated by 2.5 fold in the presence of 0.25 mM GSNO in the same condition. Previous reports [8,50] also demonstrated that catalase help with the detoxification of nitrating agents such as peroxynitrite [51]. Confocal micrographs clearly demonstrated that NO was generated only in the presence of GSNO, and there was no significant change in ROS level after GSNO treatments, indicating that all the changes observed were due to the formation of NO or nitrosative stress.

Aconitase is an important enzyme in the TCA cycle [52]. The inactivation of this protein's $[4Fe\text{-}4S]^{2+}$ cluster *may* be responsible for the repression of aconitase activity in the presence of GSNO, according to our findings. According to the evidence, oxidation of the $[4Fe\text{-}4S]^{2+}$ cluster renders it inactive due to the formation of the $[3Fe\text{-}4S]^{1+}$ paramagnetic cluster, resulting in the inactivation of aconitase [53,54]. As a result, the TCA cycle in *S. cerevisiae* was severely affected, and metabolic flux was eventually switched from the respiratory to the fermentation pathway for generation of energy. This is evident from ethanol estimation in our experimental setup, where ~1.5 fold increase in ethanol production along with elevated yield (~1.3 fold) and volumetric productivity (~1.5 fold) were observed under 0.25 mM GSNO stress conditions. From this, it can be concluded that, in the presence of GSNO-mediated nitrosative stress, the fermentation pathway may be activated in order to generate the energy required for cell survival. Then we looked into what was causing this stimulation.

A significant increase in the specific activity of ADH also supports our finding of increased ethanol production. Interestingly, it has been reported that ADH activity can be inhibited in *E. coli* in the presence of peroxynitrite, a potent nitrating agent [55]. It has also been reported that in the presence of GSNO, ADH3 can act as a stress response enzyme [24,25,56]. So we wanted to know how GSNO, as a nitrosative stress agent, modulates such biochemical changes whether through structural modification of ADH or increased expression of *adh* genes (*adh1*, *adh2* and *adh3*). To determine this, we first performed an *in vitro* assay of ADH to see if its activity changed. Interestingly, CFE treated with GSNO showed no changes in its ADH activity. This finding suggests that protein-level modification of ADH may not be possible in the presence of GSNO. As a result, we used qPCR to determine the quantitative expression levels of *adh1*, *adh2* and *adh3*. A significant 4 fold increase in *adh3* expression after GSNO treatment could be the main reason for higher enzymatic activity of ADH. However, there was no significant change in *adh1* and *adh2* expression in the presence of 0.25 mM GSNO compared to the control. This finding suggested that ADH3 activity was required to overcome the effect of GSNO stress in our experimental condition, which corroborated previous findings. According to reports, GSNO-mediated post-translational modifications such as *S*-nitrosylation of a protein can interfere with the protein-protein interactions by modulating phosphorylation, ubiquitination, acetylation, etc. [57,58]. Modulations of this type have the potential to influence cellular processes by altering the activity of various enzymes and proteins. As a result, there was a possibility that GSNO-mediated post-translational modification of important transcription factor/s would result in increased *adh3* expression [59].

Overall, these findings indicate that sub-toxic concentrations of GSNO can induce the ethanol fermentation pathway without impairing cell viability. Because the primary goal of the fermentation industry is to achieve higher yield with fewer complexities, this process clearly has potential. This method will provide a simple, cost-effective (GSNO costs are very low), and non-hazardous approach. As a result, this GSNO-treated *S. cerevisiae* will be beneficial and novel for bioethanol production. Though many methods for increasing ethanol production have been developed, this strategy may gain traction in the future. However, because it is still a laboratory phenomenon, we believe that more research is required before it can be used in industry.

7. Conclusions

According to the findings of this study, aconitase activity was suppressed in the presence of 0.25 mM GSNO, which could result in inhibition of the TCA cycle. As a result, the metabolic flux of *S. cerevisiae* was switched from respiration to fermentation, and the *adh3* gene was overexpressed. As a result, the enzymatic activity of ADH was increased, resulting in increased ethanol production. This is the first report with a higher industrial significance on the relationship between GSNO stress and ethanol production. However, more detailed research is needed to understand the underlying molecular mechanism.

Data availability

Not applicable.

Declaration of Competing Interest

The authors declare that there is no conflict of interest.

Acknowledgment

This work was supported by the University of North Bengal, West Bengal, India [Ref. No. 1514/R-2020 Dated 01.06.2020]. Authors also acknowledge Bose institute, Kolkata and Dr. KPC Life sciences, Kolkata for providing services for confocal microscopy and qPCR respectively.

Appendix A. Supplementary data

Supplementary material related to this article can be found, in the online version, at doi:https://doi.org/10.1016/j.procbio.2021.11.011.

References

[1]–[48] [illegible]

peroxynitrite reductase, J. Biol. Chem. 272 (1997) 27812–27817, https://doi.org/10.1074/jbc.272.44.27812.
[49] M.S. Choi, Pathophysiological role of S-nitrosylation and transnitrosylation depending on S-nitrosoglutathione levels regulated by S-nitrosoglutathione reductase, Biomol. Ther. 26 (2018) 533–538, https://doi.org/10.4062/biomolther.2018.179.
[50] R. Sahoo, A. Bhattacharjee, U. Majumdar, et al., A novel role of catalase in detoxification of peroxynitrite in S. cerevisiae, Biochem. Biophys. Res. Commun. 385 (2009) 507–511, https://doi.org/10.1016/j.bbrc.2009.05.085.
[51] L. Gebicka, J. Didik, Catalytic scavenging of peroxynitrite by catalase, J. Inorg. Biochem. 103 (2009) 1375–1379, https://doi.org/10.1016/j.jinorgbio.2009.07.011.
[52] C. Auger, J. Lemire, D. Cecchini, et al., The metabolic reprogramming evoked by nitrosative stress triggers the anaerobic utilization of citrate in Pseudomonas fluorescens, PLoS One 6 (2011), e28469, https://doi.org/10.1371/journal.pone.0028469.
[53] L. Castro, V. Tórtora, S. Mansilla, et al., Aconitases: non-redox iron-sulfur proteins sensitive to reactive species, Acc. Chem. Res. 52 (2019) 2609–2619, https://doi.org/10.1021/acs.accounts.9b00150.
[54] D. Han, R. Canali, J. Garcia, et al., Sites and mechanisms of aconitase inactivation by peroxynitrite: modulation by citrate and glutathione, Biochem. 44 (2005) 11986–11996, https://doi.org/10.1021/bi0509393.
[55] J.P. Crow, J.S. Beckman, J.M. McCord, Sensitivity of the essential zinc-thiolate moiety of yeast alcohol dehydrogenase to hypochlorite and peroxynitrite, Biochem. 34 (1995) 3544–3552, https://doi.org/10.1021/bi00011a008.
[56] N.H. Chen, K.Y. Djoko, F.J. Veyrier, et al., Formaldehyde stress responses in bacterial pathogens, Front. Microbiol. 7 (2016) 257, https://doi.org/10.3389/fmicb.2016.00257.
[57] M.V. Navarro, A. Chaves, D.G. Castillo, et al., Effect of nitrosative stress on the S-nitroso-proteome of Paracoccidioides brasiliensis, Front. Microbiol. 11 (2020) 1184, https://doi.org/10.3389/fmicb.2020.01184.
[58] D.T. Hess, J.S. Stamler, Regulation by S-nitrosylation of protein post-translational modification, J. Biol. Chem. 287 (2012) 4411–4418, https://doi.org/10.1074/jbc.R111.285742.
[59] Y. Sha, H.E. Marshall, S-nitrosylation in the regulation of gene transcription, Biochim. Biophys. Acta 1820 (2012) 701–711, https://doi.org/10.1016/j.bbagen.2011.05.008.

BHATTACHARJEE ARINDAM (Orcid ID: 0000-0003-0853-9513)

Variation in glucose metabolism under acidified sodium nitrite mediated nitrosative stress in *Saccharomyces cerevisiae*

Running title: Nitrosative stress in *Saccharomyces cerevisiae*

Swarnab Sengupta[1], Rohan Nath[1], Rajabrata Bhuyan[2], Arindam Bhattacharjee[1#]

1 Department of Microbiology, University of North Bengal

Corresponding author: Department of Microbiology, University of North Bengal, West Bengal, India, pin-734013, Mobile no. +919674665722, Fax no. 0353-2776319, abmicrobio@nbu.ac.in

2 Department of Bio-Science and Biotechnology, Banasthali Vidyapith (Deemed) University, Banasthali, Rajasthan, India, Pin-304022

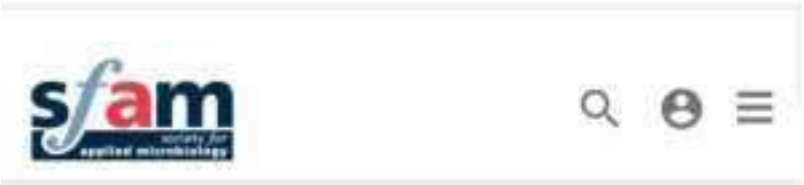

Journal of Applied Microbiology / Accepted Articles

ORIGINAL ARTICLE

Variation in glucose metabolism under acidified sodium nitrite mediated nitrosative stress in *Saccharomyces cerevisiae*

Swarnab Sengupta, Rohan Nath, Rajabrata Bhuyan, Arindam Bhattacharjee

First published: 15 June 2022

https://doi.org/10.1111/jam.15669

Abstract

Aims

The work aimed to understand the important changes during glucose metabolism in *Saccharomyces cerevisiae* under acidified sodium nitrite (ac.$NaNO_2$) mediated nitrosative stress.

Methods and Results

Confocal microscopy and FACS analysis were performed to investigate the generation of reactive nitrogen and oxygen species and redox homeostasis under nitrosative stress was also characterized. qPCR analysis revealed that the expression of *ADH* genes were upregulated under such condition whereas the *ACO2* gene was downregulated. Some of the enzymes of tricarboxylic acid (TCA) cycle were partially inhibited whereas malate metabolism and alcoholic fermentation were increased under nitrosative stress. Kinetics of ethanol production was also characterized. Network analysis was conducted to validate our findings. In presence of ac.$NaNO_2$, *in vitro* protein tyrosine nitration (PTN) formation was checked by western blotting using pure alcohol dehydrogenase (ADH) and aconitase.

Conclusions

Alcoholic fermentation rate was increased under stress condition and this altered metabolism might be conjoined with the defense machinery to overcome the nitrosative stress.

Significance and impact of the study

This is the first work of this kind where the role of metabolism under nitrosative stress has been characterized in *S. cerevisiae* and it will provide a base to develop an alternative method of industrial ethanol production.

Keywords

Tricarboxylic acid (TCA) cycle, Malate metabolism, Alcoholic fermentation, Protein tyrosine nitration

Introduction

Nitrosative stress is an *in vivo* hostile condition which is created due to the "noxious" activity of reactive nitrogen species (RNS) **(Yoshikawa *et al.* 2016)**. RNS are formed during the reaction between reactive oxygen species (ROS) and nitric oxide (NO) **(Ridnour *et al.* 2004; Peluffo and Radi 2007)**. Alteration of the redox homeostasis along with the modification of macromolecules like DNA, proteins, lipids are considered to be the major consequences of nitrosative stress that leads to the modification of physicochemical properties of the cell **(Kurutas 2016; Patra *et al.* 2019; Patra *et al.* 2017; Carballal *et al.* 2014)**. Under nitrosative stress, this structural modification of proteins and enzymes by protein tyrosine nitration (PTN) and *S*-nitrosylation may result in the alteration of their activity. Hence, PTN and *S*-nitrosylation are considered as markers of nitrosative stress **(Bartesaghi and Radi 2018; Wang *et al.* 2014; Barbosa-Sicard *et al.* 2009)**. These modifications of the proteins may affect the 'normal' cellular functions like iron metabolism, aerobic respiration etc. **(Bartesaghi and Radi 2018; Wang *et al.* 2014; Barbosa-Sicard *et al.* 2009; Witkiewicz-Kucharczyk *et al.* 2020)**. To overcome such condition, cells have different defense strategies to detoxify the effect of RNS like stimulating stress response enzymes glutathione reductase (GR), catalase, superoxide dismutase (SOD) etc. as well as non-enzymatic (GSH, NADH etc.) responses. This induction of enzymatic and non-enzymatic response under stress conditions may cause alteration in the cellular responses for the survival of the organisms **(Bartesaghi and Radi 2018; Navarro *et al.* 2020; Lindemann C *et al.* 2013; Aquilano K *et al.* 2014; Pollak N *et al.* 2007)**.

Saccharomyces cerevisiae is one of the most extensively studied organism in the field of nitrosative stress **(Bhattacharjee *et al.* 2010; Liu L *et al.* 2000; Horan *et al.* 2006; Anam *et al.* 2020)**. Previous studies showed that the growth of *S. cerevisiae* was not significantly decreased in the presence of sub-toxic dose or lower concentration of RNS **(Ying *et al.* 2017; Nasuno R *et al.* 2014; Peláez-Soto *et al.* 2020)**. It has also been reported that the function of the respiratory chain in *S. cerevisiae* may get hampered under nitrosative stress due to the inactivation of several TCA cycle enzymes. One important enzyme of this cycle, aconitase, catalyzes the reaction from citrate to isocitrate, and is also a well-known marker of redox stress **(Lushchak *et al.* 2014)**. Previous reports suggest that it can be affected under nitrosative insult **(Radi 2018; Lushchak *et al.* 2010)**. Thus, ATP synthesis may get inhibited under such condition **(Ying *et al.* 2017; Sahoo *et al.* 2003)**. However, the exact mechanism of generation of energy as well as the citrate metabolism under such condition has not been well characterized. Earlier studies from our lab showed upregulation of ADH activity and higher

ethanol production under ac.$NaNO_2$ mediated nitrosative stress using *S. cerevisiae* **(Sengupta *et al.* 2020)**. A few reports also indicated towards an increase in alcohol dehydrogenase activity under nitrosative stress **(Liu L *et al.* 2000; Jahnová *et al.* 2019; Staab *et al.* 2008)**. Hence, all these reports imply that the glucose metabolic flux may get shifted from respiration towards fermentation pathway under nitrosative stress **(Ying *et al.* 2017; Fitzsimmons *et al.* 2018; Kitichantaropas *et al.* 2016; Tillmann *et al.* 2011)**. But, definitive studies regarding the characterization of glucose metabolism in *S. cerevisiae* under nitrosative stress condition was not yet well-established that can answer those questions.

Hence, the primary objective of our work was to characterize the glucose metabolism in *S. cerevisiae* under nitrosative stress by assaying different key enzymes of the TCA cycle, alcohol fermentation, malate metabolism and anaplerotic reactions. Further we investigated the alteration in redox homeostasis by estimating the reduced to oxidized glutathione (GSH/GSSG) ratio, catalase and GR. In addition to this, *in vitro* study of the protein modification in aconitase and ADH enzymes was also performed under stress condition. Here, we have tried to delineate the metabolic pathway in *S. cerevisiae* under nitrosative stress. This study has a huge potential as application for high ethanol production at industrial scale and at the same time serves as the base to characterize the metabolic responses of *S. cerevisiae* under nitrosative stress.

Materials and Methods

Yeast culture and growth

Wild type haploid *S. cerevisiae* Y190 [ATCC 96400] (a gift from Prof. Sanjay Ghosh, Calcutta University, India), was used for all the experiments. Cells were grown for overnight in YPD (2% w/v yeast extract [HiMedia], 2% w/v peptone [HiMedia] and 2% w/v dextrose [Merck] at 30°C at 80 RPM. The strain was preserved in 50% glycerol stocks at -20°C freezer. 200 µL from the glycerol stock was inoculated in a fresh YPD broth and incubated overnight at 30°C. Streak plating was performed on YPD agar to ensure purity and a single colony was cultured overnight in YPD broth at 30°C. These cultures were used as inoculum for further experiments at an $O.D._{600}$~0.05.

Preparation of acidified sodium nitrite and determination of cell viability

A 100 mM stock solution of ac.$NaNO_2$ was prepared by adding $NaNO_2$ to 0.2 N HCl. This was used as the 'NO donor' **(Regev-Shoshani *et al.* 2013)** and applied to the culture at the early log phase ($O.D._{600}$~0.3). After 12 hours, cell viability was determined using serial dilution and growth curves were also determined based on $O.D._{600}$ for 12 hours at 60-min intervals. For the control experiment, the yeast was cultured in absence of ac.$NaNO_2$.

Preparation of cell free extract (CFE) and estimation of protein concentration

Overnight (12 hours) grown cultures of treated and untreated samples ($O.D._{600} \sim 1.8$) were centrifuged and cell pellets were mixed with lysis buffer containing 100 mM Tris-HCl pH 7.6, 150 mM NaCl, 2 mM EDTA, protease inhibitor cocktail (Sigma-Aldrich), and 1 mM PMSF and lysed by using glass beads. Concentration of protein was estimated as per the protocol of Bradford using BSA as the standard **(Bradford 1976)**.

Estimation of GSH:GSSG ratio

The GSH and GSSG concentration was determined according to the method of Akerboom et al. with slight modification **(Akerboom and Sies 1981)**. In brief, CFEs were first deproteinized with 2 M $HClO_4$, 2 mM EDTA and then neutralized with 2 M KOH containing 0.3 M HEPES pH 7.0. Half of the neutralized samples were taken to estimate the *in vivo* thiol concentration (GSH+GSSG) by GR [Sigma-Aldrich] dependent DTNB [5,5-dithio-bis(2-nitrobenzoic acid)] reduction. The other half was treated with 2-vinylpyridine (50:1 v/v) for 1 hour and used to determine the GSSG concentration by UV spectroscopy at 412 nm. Concentration of GSH and GSSG were expressed in nmol/mg of protein.

Detection of ROS and RNS

Confocal microscopy

RNS and ROS were detected by confocal microscopy (Leica TCS SP8) from Bose institute, Kolkata, as per the protocol of Invitrogen with some modifications. In brief, $2X10^6$ overnight grown cells were washed and resuspended in PBS pH 7.4 and fixed using absolute ethanol. Then, dyes (DAF-FM specific for NO and H2DCFDA specific for ROS) were added at a final concentration of 1.5 µM and incubated for 30 minutes in the dark. For confocal microscopy excitation was fixed at 495 nm and emission at 515 nm. Micrographs were captured at 45X magnification and the intensity of fluorescence was recorded using the Leica LAS X software.

FACS

FACS (BD LSRFortessa) analysis for ROS and RNS were done from IICB, Kolkata, as per the protocol of Invitrogen. Samples were prepared as mentioned above and dye-free cells were used as the blank. The photomultiplier tube voltage was kept at 190 mV for the FITC channel at a flow rate of 12 µl/min. 10000 events were recorded for each sample and histograms were prepared by plotting the cell counts against fluorescence in the FITC channel. Excitation and emission were set as above and data were analysed by using FACS Diva software.

Quantification of ethanol and reducing sugar

The concentrations of ethanol and reducing sugar were estimated as per the protocol of Zhang *et al.* with slight modifications **(Zhang P *et al.* 2019)**. In short, overnight grown untreated and

treated cultures were centrifuged at 5000 *g*, and supernatants were collected. These were mixed with an equal volume of 20% TCA at room temperature for 5 min. Following centrifugation at 10000 *g*, supernatants were treated with 1/5 volume of 20% CTAB at 65°C for 10 min and again centrifuged at 10000 *g*. Samples were diluted 100 fold and mixed with $KMnO_4$ solution and incubated at 40°C for 90 min. Initial and final O.D. were recorded at 526 nm. A standard curve for the ethanol estimation was prepared with absolute ethanol (Merck). For the reducing sugar estimation, the pretreated sample was diluted 10-fold and mixed with DNS solution, after which O.D. was recorded at 540 nm. A standard curve for reducing sugar estimation was prepared with glucose (Merck). The kinetics of ethanol production (yield and productivity) were also determined **(Mithra *et al.* 2018)**.

Enzymatic assays

All enzymatic assays were based on spectophotometric analysis. GR **(Carlberg and Mannervik 1975)** and malate synthase (MS) **(Chell *et al.* 1978)** were determined at 412 nm and catalase **(Aebi *et al.* 1984)** and aconitase **(Castro *et al.* 1994)** at 240 nm. Pyruvate carboxylase (PC) was measured after **Payne and Morris (1969)** and citrate synthase (CS) after **Srere 1971**. The other enzyme activities were determined by changes in NADH at 340 nm: pyruvate dehydrogenase (PDH), isocitrate dehydrogenase (ICDH) and malate dehydrogenase (MDH) **(Bergmeyer *et al.* 1974)**, MDH (decarboxylating) **(Geer *et al.* 1980)**, aldehyde dehydrogenase (ALDH) **(Bostian and Betts 1978)**, and pyruvate decarboxylase (PDC) **(Gounaris *et al.* 1971)**. In all cases specific activity was expressed in mU/mg of protein.

Estimation of the concentration of citrate

Intracellular and extracellular citrate concentration was determined by a citrate assay kit (Sigma-Aldrich) and expressed in ng/µL.

RNA isolation and qPCR

RNA isolation, cDNA preparation and qPCR was outsourced to Dr. KPC Life sciences, India. For this, treated and untreated samples were centrifuged at 5000 *g* and after two wash steps with PBS, RNA was isolated by use of standard affinity columns and eluted in nuclease-free water. 500 ng of RNA was used as the template for cDNA synthesis which was performed with 200 units of reverse transcriptase (RT) enzyme (Thermo Scientific) in RT buffer containing 10 mM dNTPs and 10 µM random hexamer. Following incubated at 42°C for 60 min and heat inactivation at 65°C for 15 min. The cDNA was used for +RT qPCR (Biorad CFX-96) using SUPERZym qPCR master mix (Dr. KPC Life sciences). The Diluted RNA sample was used as the template for (-RT) qPCR. A negative control (NTC) was set up without template. The two-step PCR was initiated with denaturation at 95°C for 15 sec and annealing and extension

was done at 60°C for 30 sec for 40 cycles, followed by a melt curve. The primers for the experimental and housekeeping genes were designed from NCBI and enlisted in **Table S1**.

Functional annotation and network analysis

The enzymes, with altered activity in presence of 0.5 mM ac.$NaNO_2$, were subjected for functional enrichment analysis. First, the STRING database was used to screen interactions followed by creating a functionally interacting network **(Szklarczyk *et al.* 2019)**. Few closely associated enzymes were added to the network to increase stability and obtain reliable predictions. The networks were analyzed and visualized using Cytoscape (Version 3.7) **(Shannon *et al.* 2003)**. Annotation of functionally activated and deactivated enzymes were analyzed using Gene Ontology (GO) analysis by DAVID (Database for Annotation, Visualization and Integrated Discovery) **(Dennis *et al.* 2003)**. Enzyme sets were taken from respective networks, and their annotations classified into biological process (BP), cellular component (CC) and molecular function (MF). For the GO analyses, Bonferroni correction method was used to identify significant terms associated with the genes and the error rates was reduced by removing the false discovery outcomes from any prediction.

Western blotting

Western blots were produced from 10% polyacrylamide gels **(Laemmli *et al.* 1970)** loaded with the pure enzymes aconitase (Sigma-Aldrich) and ADH (Sigma-Aldrich). Following transfer to PVDF membranes the blots were probed with anti 3-nitrotyrosine monoclonal antibody (Sigma-Aldrich) at 1:1000 dilution in TBST and following incubation with HRP conjugated goat anti-mouse IgG secondary antibody (Sigma-Aldrich) at 1:10000 dilution in TBST, bands were visualized by using chemiluminescence reagent (Abcam). Images were captured using DNR bio-imaging system miniBIS Pro (USA) with GelQuant Express Analysis Software.

Condition of stress and assays with pure aconitase and alcohol dehydrogenase

Pure protein (200 µg) was incubated for 30 min at room temperature in presence of different concentrations (0.1 mM, 0.3 mM, 0.5 mM) of ac.$NaNO_2$ and 0.1 mM peroxynitrite (positive control). An aliquot of 80 µg was used to determine PTN by western blotting as described above. The rest was used for specific activity determination described above.

Statistical analysis

Experimental data were statistically analyzed by using two tailed paired T-test and expressed as mean±SD. Level of significance (p) ≤ 0.01 was considered as significant. Most of the experiments were performed at least in triplicate.

Results

Effect of acidified sodium nitrite on redox homeostasis

The growth curves of *S. cerevisiae* (Fig. S1), were similar between control and 0.5 mM ac.$NaNO_2$ treated *S. cerevisiae* with a growth rate of 0.22 hr^{-1} for both, indicating that the used concentration of ac.$NaNO_2$ was not toxic to the cells. The redox homeostasis of treated and untreated cells was assessed by GSH/GSSG ratio, GR activity and catalase activity. The GSH/GSSG ratio was increased by 4.2 fold under the stress condition as compared to the control (Fig. 1A). There was no significant change in total glutathione concentration but the concentration of GSSG was decreased by 2.3 fold (Fig. S2A) whereas concentration of GSH was increased 1.8 fold (Fig. S2B) in treated cells. In addition, GR activity was increased by 4 fold under the stress condition (Fig. 1B). Activity of catalase was also increased, by approximately 2.4 fold under the stress condition as compared to the control (Fig. 1B). These findings suggest that the redox homeostasis of the cells were significantly altered under the stress condition and the cells were trying to compensate and adapt. To study the alteration of redox homeostasis, the generation and accumulation of ROS and RNS within the cell was investigated by confocal microscopy (Fig.2A-J) and FACS (Fig. 2K-N). The result showed that ROS was generated in both treated and untreated cells with no significant change, while, RNS generation was only observed in the 0.5 mM ac.$NaNO_2$ treated cells (79%), clearly suggesting that the changes observed in the treated cells were solely due to the generation of RNS. This data is corroborated with our previously published report **(Sengupta *et al.* 2020)**.

Effect of acidified sodium nitrite on kinetics of ethanol production

The effect of 0.5 mM ac.$NaNO_2$ on the ethanol yield and productivity was next determined. We found that ethanol yield was increased by 1.2 fold and consumption of sugar was ~14% higher under the stress condition. The volumetric productivity was increased, by approximately 1.3 fold in the presence of 0.5 mM ac.$NaNO_2$. 69% of the theoretical ethanol yield was achieved during treatment whereas only 59% of the theoretical ethanol yield was achieved in control (Table 1). These results clearly indicated that alcoholic fermentation rate was increased under ac.$NaNO_2$ mediated nitrosative stress. Next, we checked the effect of 0.5 mM ac.$NaNO_2$ on the TCA cycle and other biochemical pathways, for which activity of some of the key enzymes were determined.

Effect of acidified sodium nitrite on key enzymes of important biochemical pathways

The specific activity of aconitase was approximately 50% less in treated cells as compared to the control (Fig. 3A) and the combined concentration of intracellular and extracellular citrate

was also halved (Table S2), indicating that the synthesis of citrate was decreased under stress condition (Fig. 3B). Hence, we assayed the activity of CS and this was also found to be decreased by 50% (Fig. 3A), suggesting that the citrate metabolism as well as the TCA were affected. As the specific activity of CS was significantly reduced, the utilization of pyruvate was next assessed. Pyruvate is the end product of glycolysis and is an important secondary metabolite that is further utilized in the TCA cycle, either by formation of acetyl-CoA or OAA by the activity of PDH or PC, respectively **(Voet and Voet 1995)**. Interestingly, it was found that the specific activity of PDH and PC were lowered by approximately 50% and 15%, respectively, under the stress condition as compared to the control (Fig. 3A). The fate of OAA in TCA cycle needed to be established, for which we measured the activity of MDH as it catalyzes the reversible conversion from OAA to malate. Interestingly, activity of MDH was increased by approximately 1.3 fold under the stress condition (Fig. 3A). All these results indicated that the TCA cycle was amortized under the stress condition, but the higher activity of MDH implied that the concentration of malate might be increased in presence of 0.5 mM ac.$NaNO_2$. In combination with elevated ethanol production, this pointed towards increased pyruvate concentration within the cells under nitrosative stress. This was confirmed by measuring the activity of MDH (decarboxylating), that catalyzes the conversion from malate to pyruvate. Here, the activity of this enzyme was 1.3 fold increased in the treated cells (Fig. 3A). Furthermore, we assessed the specific activity of PDC and this was sharply increased by 3.2 fold (Fig. 3A). A drop of approximately 50% in the specific activity of ICDH was also observed under the stress condition (Fig. 3A). Based on these findings, we hypothesized that the TCA cycle was partially inhibited under the stress condition. Thus, we also determined the activity of ALDH, an important enzyme for the PDH-bypass pathway **(Remize *et al.* 2000)**. The activity of this enzyme was found to be decreased by 64% as compared to the control (Fig. 3A). Along with this, the activity of MS, an important enzyme of glyoxylate shunt (an anaplerotic variant of TCA cycle) **(Chew *et al.* 2019)**, was decreased by approximately 40 % in 0.5 mM ac.$NaNO_2$ treated *S. cerevisiae* cells (Fig. 3A).

Network and functional annotation studies with the altered protein activities

To validate our findings obtained from the biochemical enzymatic assays, we investigated the effect of nitrosative stress on different metabolic enzymes of *S. cerevisiae* using bioinformatics. Under nitrosative stress, the enzymes with altered activity were subjected to a network analysis and functional annotation studies. Of the activated enzymes, MDH and PDC predominantly participated in the network with a maximum number of connections (Fig. 4A). Due to the increased activity of these enzymes, the yeast cellular system was predicted to be involved

primarily in the biological processes of pyruvate and malate metabolism, and in gluconeogenesis (Table 2). The network formed by enzymes with decreased activity contained CS, isocitrate lyase, PDH, and aconitase with maximum connectivity (Fig. 4B). The terms for predicted biological processes with these enzymes were TCA cycle, glyoxylate cycle, and biosynthesis of glutamate and acetate. In terms of cellular location, most of the enzymes were predicted to be located in the mitochondria. Additionally, the most enriched molecular functions were predicted to be MDH activity and ADH (NAD) activity due to the activated enzymes in the treated yeast cells. On the other hand, the ALDH activity, transferase activity, transferring acyl groups, acyl groups converted into alkyl on transfer, and lyase activity might be reduced due to the decreased activity of enzymes participating in these functions (Table 2).

Effect of acidified sodium nitrite on *ADH* and *ACO* genes expression

As we found that ethanol production and ADH activity had increased and aconitase activity had decreased in the presence of 0.5 mM ac.$NaNO_2$, we assessed the expression of *ADH* and *ACO* genes. As Fig. 5 shows, expression of *ADH1*, *ADH2* and *ADH3* were increased by, ~2.1 fold, ~2.4 fold, and ~3.5 fold respectively, under the stress condition as compared to the control. Expression of *ACO2* was almost 50% lower in treated cells as compared to the control. Surprisingly, the expression of *ACO1* was found to be increased by 1.2 fold in treated cell in comparison to the control (Table S3-S7, Fig. 5).

***In vitro* Protein tyrosine nitration (PTN) study with pure aconitase and ADH**

As variation in glucose metabolism was observed with a significant upregulation of ADH and downregulation of aconitase, we assessed the protein tyrosine nitration (PTN) formation for these two enzymes. PTN formation was observed in aconitase following treatment with 0.3 mM and 0.5 mM ac.$NaNO_2$ but not with 0.1 mM ac.$NaNO_2$ treated aconitase or without treatment. The specific activity of aconitase was gradually reduced with the of higher concentrations of treatment of ac.$NaNO_2$. The reduction in aconitase activity was maximal for the positive control of 0.1 mM peroxynitrite treatment (Fig. 6A). Different results were obtained with pure ADH. PTN formation was only observed in 0.1 mM peroxynitrite treated ADH, while it was absent as a result of ac.$NaNO_2$ treatment. The specific activity of ADH remained unaltered in ac.$NaNO_2$ treated samples but drastically decreased in 0.1 mM peroxynitrite treated ADH as compared to the untreated ADH (Fig. 6B).

Discussion

In this present study, we demonstrate variation in glucose metabolism in *S. cerevisiae* under nitrosative stress that is mediated by 0.5 mM ac.$NaNO_2$. Results from FACS and confocal microscopy confirmed that ROS was equally produced in both treated and untreated cells, but

RNS was generated only in the presence of ac.$NaNO_2$. Hence, the observed phenomena were due to the nitrosative stress under our experimental condition. Changes in the redox homeostasis is a key marker of nitrosative stress **(Kurutas 2016; Maciejczyk *et al.* 2022)**. Under our experimental condition, an increased GSH/GSSG ratio, elevated concentration of GSH and reduced concentration of GSSG were observed, that in combination suggest that the treated cells responded by raising the intracellular reduced equivalent in the form of GSH **(Astuti *et al.* 2016)**. GSH is a well-known stress response component that helps to combat reactive-species mediated damage (**Aquilano K *et al.* 2014**). Previous reports have also suggested that the declined level of GSH may induce deleterious activity of NO in the form of DNA damage and protein modification **(Aquilano K *et al.* 2014; Kalinina and Novichkova 2021; Lei *et al.* 2016; Sies *et al.* 1997; Forman *et al.* 2009)**. This observation was corroborated with the higher activity of GR which catalyzes the conversion of GSSG to GSH under stress **(Forman *et al.* 2009)**. Though reported data suggests that GR activity can be inhibited in *Schizosaccharomyces pombe* under the peroxynitrite mediated nitrosative stress **(Saboo *et al.* 2006)**, Navarro *et al.* recently reported that GR activity can be stimulated in the presence of NO **(Navarro *et al.* 2020)**. Here, we also found a sharp increase in GR activity in presence of 0.5 mM ac. $NaNO_2$. Thus, it can be concluded that GSSG was converted to GSH by the activity of GR to maintain the redox homeostasis under our experimental condition. In addition, activity of catalase, an important stress response enzyme **(Patra *et al.* 2019)**, was also increased in the treated cells, and this might be involved to detoxify reactive species that were generated by the action of ac.$NaNO_2$ **(Navarro *et al.* 2020; Bhattacharjee *et al.* 2010; Gebicka and Didik 2009; Saboo *et al.* 2009)**.

In *S. cerevisiae* ADH1, ADH3, ADH4, and ADH5 produce ethanol from acetaldehyde whereas ADH2 is involved in the reverse reaction i.e. production of acetaldehyde from ethanol. It can be expected, that the elevated expression of *ADH1* and *ADH3* genes under the stress condition resulted in higher enzyme activity and this most likely contributed to higher ethanol production. That expression of *ADH2* was induced under stress condition might be due to the higher ethanol production. This enzyme can assist in generation of reducing equivalents in the form of NADH and maintain the redox status of the cell **(Maestre *et al.* 2008)**. Though *S. cerevisiae* is a crabtree-positive organism **(Pfeiffer *et al.* 2014)**, the increased percentages of theoretical ethanol yield, higher rate of sugar utilization indicated that the fermentation rate under the stress condition was upregulated. Overall, these results suggested a probable metabolic reprogramming towards fermentation. In addition, we found that the activity of PDH, CS, aconitase, ICDH were reduced in treated cells, clearly indicating a partial blocking of the

TCA cycle. These results are in line with earlier reports which showed the downregulation of mitochondrial proteins, mainly the TCA cycle enzymes, under nitrosative stress **(Auger *et al.* 2011; Abello *et al.* 2009)**. The activity of CS is considered as a marker of mitochondrial function, and the reduction in its specific activity suggested that the mitochondrion was highly affected in the presence of 0.5 mM ac.$NaNO_2$ **(Borys *et al.* 2019)**. This was also supported by the higher expression of *ACO1*. The product of that gene not only catalyzes the conversion from citrate to isocitrate **(Staab *et al.* 2008)**, but is also involved in certain unrelated cellular processes, thus acting as a moonlighting protein **(Gancedo *et al.* 2016)**. One of the important functions of ACO1p is to maintain the integrity of mitochondrial DNA **(Gancedo *et al.* 2016; Chen *et al.* 2007; Yazgan and Krebs 2012)**. Hence, the higher expression of the *ACO1* indicated that the mitochondrial activity might be affected under the stress conditions we applied. Unlike *ACO1*, the gene expression of *ACO2* was reduced and overall specific activity of aconitase was dropped by 50%, suggesting that ac.$NaNO_2$ might affect transcription of aconitase. A model of glucose metabolism in *S. cerevisiae* in the presence of 0.5 mM ac.$NaNO_2$ is proposed in Fig. 7. The rate limiting enzyme of the TCA cycle is ICDH, which catalyzes the conversion from isocitrate to α-ketoglutarate **(Voet and Voet 1995)**, and this enzyme activity was decreased, together with that of PDH, which catalyzes the conversion from pyruvate to acetyl CoA **(Voet and Voet 1995)**. This explains the observed reduction in citrate metabolism. Other reports have also suggested that the activity of PDH and ICDH can be affected under nitrosative and oxidative stress **(Auger *et al.* 2011; Ferrer-Sueta G *et al.* 2018)**. Formation of acetyl CoA from pyruvate is the key step for utilizing glucose via respiration pathway **(Voet and Voet 1995)**, but acetyl-CoA can also be synthesized via the PDH-bypass pathway, a PDH-independent alternative route which requires the activity of PDC and ALDH among the other enzymes **(Remize *et al.* 2000)**. Though the activity of PDC [also a crucial enzyme of the fermentation pathway **(Voet and Voet 1995)**] was found to be increased, the activity of ALDH [oxidizes acetaldehyde to acetate **(Remize *et al.* 2000)**] was decreased under the stress condition. Reduction in ALDH activity might affect the acetyl-CoA production. In addition, activity of MS was decreased as a result of treatment, which might be due to the lower availability of acetyl-CoA. Reduced activity of MS might also affect the glyoxylate cycle, an anaplerotic variant of the TCA cycle present in *S. cerevisiae* **(Chew *et al.* 2019)**. Acetyl-CoA is also a positive allosteric modulator of PC, an important anaplerotic enzyme that replenishes the intermediates of TCA cycle by catalyzing the reaction from pyruvate to oxaloacetic acid **(Voet and Voet 1995, Adina-Zada *et al.* 2012)**. Any depletion in the production of acetyl-CoA under our experimental condition might be interfering with the activity of PC **(Voet and**

Voet 1995; Adina-Zada *et al.* 2012). Hence, all these results suggested that the requirement for replenishing the intermediates of the TCA cycle might be reduced in presence of ac.$NaNO_2$, indicating a partial blocking of the TCA cycle under the stress condition.

The detected elevated specific activity of MDH and MDH (decarboxylating) enzymes under the stress condition are very interesting as this observation suggests that, under the stress condition, OAA formed by PC was rerouted to pyruvate via formation of malate. It has been reported that OAA cannot cross the mitochondrial membrane but malate can **(Voet and Voet 1995)**. Reports suggest that the affinity of MDH (decarboxylating) is very low (K_m = 50 mM) but malate metabolism as well as activity of the MDH (decarboxylating) may be induced during the adverse conditions like starvation in *S. cerevisiae* **(Redzepovic *et al.* 2003)**. MDH (decarboxylating) also contributes to the generation of intracellular flux of NADPH **(Knuf *et al.* 2013)** that plays a major role in the protection against oxidative stress and also participates in different biological processes **(Pollak *et al.* 2007)**, suggesting a possible stress response activity of MDH (decarboxylating). On the other hand, activity of MDH is also very important to generate cytosolic NADH, an important component of energy metabolism and an antioxidant cofactor **(Voet and Voet 1995; Miyagi *et al.* 2009)**. Therefore, it is likely that under the stress condition, when the energy generation via TCA cycle was heavily compromised, upregulation of MDH and MDH (decarboxylating) helped to generate energy intermediates which in turn caused the rerouting of glucose metabolic flux towards fermentation. Again, higher activity of MDH (decarboxylating) has been also reported during alcoholic fermentation in *S. cerevisiae* **(Redzepovic *et al.* 2003)**. This enzyme can be strongly increased during the switching from respiration to fermentation in *S. cerevisiae* **(Xiao *et al.* 2018)**. We further observed increases in the activity of PDC and ADH, suggesting a higher rate of ethanol fermentation. Thus, a metabolic reprogramming towards fermentation might have taken place in the presence of ac.$NaNO_2$ in *S. cerevisiae*.

The experimental results were supported by bioinformatics analyses where fermentation was predicted as strongly activated, in combination with elevated malate metabolic metabolism. In contrast, the TCA cycle and glyoxylate shunt were predicted to be slowed down under the stress condition, confirming that variation in glucose metabolism in *S. cerevisiae* during nitrosative stress. The metabolic reprogramming might not only be involved in energy generation but also seemed to be a part of the stress response. This reprogrammed glucose metabolism was coupled with the antioxidant machinery of the cell, which in combination were able to maintain the cell viability to almost unaltered levels in 0.5 mM ac.$NaNO_2$ treated culture as compared to the control.

In vitro study of PTN was further carried out with pure aconitase and ADH. PTN is one of the important marker of redox stress **(Corpas *et al.* 2009; Cipak Gasparovic *et al.* 2017)**. As mentioned earlier, aconitase is very sensitive to redox stress **(Radi 2018; Lushchak *et al.* 2010)**. Aconitase contains a 4Fe-4S cluster in its active site **(Frick and Wittmann 2005)** and this is very prone to oxidation that leads to its inactivation **(Radi 2018; Wachnowsky *et al.* 2019; Fridovich 2003)**. Treatment with 0.3 and 0.5 mM ac.$NaNO_2$ produced a positive signal for PTN and reduced the specific activity of the treated enzyme. Tyrosine nitration increases the negative charge of the protein and also adds comparatively bulky substituents that in combination may alter local charge distribution as well as the protein configuration **(Radi 2018)**. This explains the partial inhibition of aconitase. However, ac.$NaNO_2$ treatment was not able to induce the formation of PTN in ADH. This enzyme remained unaltered without a change in western blots or specific activity, suggesting that ac.$NaNO_2$ could not affect the activity of the ADH via PTN formation.

In conclusion, our findings reveal that the nefarious activity of acidified sodium nitrite was substantially reduced by metabolic reprogramming towards fermentation, conjoined with the anti-oxidant defense system. This study provides insight into the variation in glucose metabolism in *S. cerevisiae* under acidified sodium nitrite mediated nitrosative stress and contributes to a better understanding of the mechanistics behind the process.

Acknowledgement

Authors acknowledge University of North Bengal for providing infrastructure and research project fund to carry out the research. Authors also acknowledge IICB, Kolkata, Bose institute, Kolkata and Dr. KPC Life sciences, Kolkata for providing the paid-services for FACS, confocal microscopy and qPCR respectively.

Conflict of interest

No conflict of interest declared.

Authors' contributions

AB & SS Designed the experiments. SS & RN Performed the wet lab experiments and artwork preparation. RB Designed and Performed the network analysis. AB & SS analyzed the data and wrote the manuscript. All the authors read the manuscript and approved it for the submission.

Availability of data and material

Data available upon reasonable request.

References

Abello, N., Kerstjens, H.A., Postma, D.S., Bischoff, R. (2009) Protein tyrosine nitration: selectivity, physicochemical and biological consequences, denitration, and proteomics

methods for the identification of tyrosine-nitrated proteins. *J Proteome Res* **8**, 3222-38. https://doi.org/10.1021/pr900039c

Adina-Zada, A., Zeczycki, T.N., Attwood, P.V. (2012). Regulation of the structure and activity of pyruvate carboxylase by acetyl CoA. *Arch Biochem Biophys* **519**, 118-30. https://doi.org/10.1016/j.abb.2011.11.015

Aebi, H. (1984) Catalase in vitro. *Methods Enzymol* **105**, 121-6. https://doi.org/10.1016/s0076-6879(84)05016-3

Akerboom, T.P., Sies, H. (1981) Assay of glutathione, glutathione disulfide, and glutathione mixed disulfides in biological samples. *Methods Enzymol* **77**, 373-82. https://doi.org/10.1016/s0076-6879(81)77050-2

Anan, K., Nasuno, R., Takagi, H. (2020) A novel mechanism for nitrosative stress tolerance dependent on GTP cyclohydrolase II activity involved in riboflavin synthesis of yeast. *Sci Rep* **10**, 6015. https://doi.org/10.1038/s41598-020-62890-3

Aquilano, K., Baldelli, S., Ciriolo, M.R. (2014) Glutathione: new roles in redox signaling for an old antioxidant. Front Pharmacol **5**, 196. https://doi.org/10.3389/fphar.2014.00196

Astuti, R.I., Nasuno, R., Takagi, H. (2016) Nitric oxide signaling in yeast. *Appl Microbiol Biotechnol* **100**, 9483-9497. https://doi.org/10.1007/s00253-016-7827-7

Auger, C., Lemire, J., Cecchini, D., Bignucolo, A., Appanna, V.D. (2011) The metabolic reprogramming evoked by nitrosative stress triggers the anaerobic utilization of citrate in *Pseudomonas fluorescens*. *PLoS One* **6**, e28469. https://doi.org/10.1371/journal.pone.0028469

Barbosa-Sicard, E., Frömel, T., Keserü, B., Brandes, R.P., Morisseau, C., Hammock, B.D., Braun, T., Krüger, M., Fleming, I. (2009) Inhibition of the soluble epoxide hydrolase by tyrosine nitration. *J Biol Chem* **284**, 28156-28163. https://doi.org/10.1074/jbc.M109.054759

Bartesaghi, S., Radi, R. (2018) Fundamentals on the biochemistry of peroxynitrite and protein tyrosine nitration. *Redox Biol* **14**, 618-625. https://doi.org/10.1016/j.redox.2017.09.009

Bergmeyer, H.U., Gawehn, K., Grassl, M. (1974) Methods of enzymatic analysis. Weinheim: Verlag Chemie, Academic Press. New York.

Bhattacharjee, A., Majumdar, U., Maity, D., Sarkar, T.S., Goswami, A.M., Sahoo, R., Ghosh, S. (2010) Characterizing the effect of nitrosative stress in *Saccharomyces cerevisiae*. *Arch Biochem Biophys* **496**,109-16. https://doi.org/10.1016/j.abb.2010.02.003

Borys, J., Maciejczyk, M., Antonowicz, B., Krętowski, A., Sidun, J., Domel, E., Dąbrowski, J.R., Ładny, J.R., Morawska, K., Zalewska, A. (2019) Glutathione metabolism, mitochondria activity, and nitrosative stress in patients treated for mandible fractures. *J Clin Med* **8**, 127. https://doi.org/10.3390/jcm8010127

Bostian, K.A., Betts, G.F. (1978) Kinetics and reaction mechanism of potassium-activated aldehyde dehydrogenase from *Saccharomyces cerevisiae*. *Biochem J* **173**, 787-98. https://doi.org/10.1042/bj1730787

Bradford, M.M. (1976) A rapid and sensitive method for the quantitation of microgram quantities of protein utilizing the principle of protein-dye binding. *Anal Biochem* **72**, 248-54. https://doi.org/10.1006/abio.1976.9999

Carballal, S., Bartesaghi, S., Radi, R. (2014) Kinetic and mechanistic considerations to assess the biological fate of peroxynitrite. *Biochim Biophys Acta* **1840**, 768-80. https://doi.org/10.1016/j.bbagen.2013.07.005

Carlberg, I., Mannervik, B. (1975) Purification and characterization of the flavoenzyme glutathione reductase from rat liver. *J Biol Chem* **250**, 5475-80. https://doi.org/10.1016/S0021-9258(19)41206-4

Castro, L., Rodriguez, M., Radi, R. (1994) Aconitase is readily inactivated by peroxynitrite, but not by its precursor, nitric oxide. *J Biol Chem* **269**, 29409-15. https://doi.org/10.1016/S0021-9258(18)43894X

Chell, R.M., Sundaram, T.K., Wilkinson, A.E. (1978) Isolation and characterization of isocitratelyase from a thermophilic *Bacillus* sp. *Biochem J* **173**, 165-77. https://doi.org/10.1042/bj1730165

Chen, X.J., Wang, X., Butow, R.A. (2007) Yeast aconitase binds and provides metabolically coupled protection to mitochondrial DNA. *Proc Natl Acad Sci USA* **104**, 13738-43. https://doi.org/10.1073/pnas.0703078104

Chew, S.Y., Chee, W.J.Y., Than, L.T.L. (2019) The glyoxylate cycle and alternative carbon metabolism as metabolic adaptation strategies of *Candida glabrata*: perspectives from Candida albicans and Saccharomyces cerevisiae. *J Biomed Sci* **26**, 52. https://doi.org/10.1186/s12929-019-0546-5

Cipak Gasparovic, A., Zarkovic, N., Zarkovic, K., Semen, K., Kaminskyy, D., Yelisyeyeva, O., Bottari, S.P. (2017) Biomarkers of oxidative and nitro-oxidative stress: conventional and novel approaches. *Br J Pharmacol* **174**, 1771-1783. https://doi.org/10.1111/bph.13673

Corpas, F.J., Chaki, M., Leterrier, M., Barroso, J.B. (2009) Protein tyrosine nitration: a new challenge in plants. *Plant Signal Behav* **4**, 920-3. https://doi.org/10.4161/psb.4.10.9466

Dennis, G.Jr., Sherman, B.T., Hosack, D.A., Yang, J., Gao, W., Lane, H.C., Lempicki, R.A. (2003) DAVID: database for annotation, visualization, and integrated discovery. *Genome Biol* **4**, P3. https://doi.org/10.1186/gb-2003-4-9-r60

Ferrer-Sueta, G., Campolo, N., Trujillo, M., Bartesaghi, S., Carballal, S., Romero, N., Alvarez, B., Radi, R. (2018) Biochemistry of peroxynitrite and protein tyrosine nitration. *Chem Rev* **118**, 1338-1408. https://doi.org/10.1021/acs.chemrev.7b00568

Fitzsimmons, L., Liu, L., Porwollik, S., Chakraborty, S., Desai, P., Tapscott, T., Henard, C., McClelland, M., Vazquez-Torres, A. (2018) Zinc-dependent substrate-level phosphorylation powers Salmonella growth under nitrosative stress of the innate host response. *PLoS Pathog* **14**, e1007388. https://doi.org/10.1371/journal.ppat.1007388

Forman, H.J., Zhang, H., Rinna, A. (2009) Glutathione: overview of its protective roles, measurement, and biosynthesis. *Mol Aspects Med* **30**, 1-12. https://doi.org/10.1016/j.mam.2008.08.006

Frick, O., Wittmann, C. (2005) Characterization of the metabolic shift between oxidative and fermentative growth in *Saccharomyces cerevisiae* by comparative 13C flux analysis. *Microb Cell Fact* **4**, 30. https://doi.org/10.1186/1475-2859-4-30

Fridovich, I. (2003) With the help of giants. *Annu Rev Biochem* **72**, 1-18. https://doi.org/10.1146/annurev.biochem.72.081902.140918

Gancedo, C., Flores, C.L., Gancedo, J.M. (2016) The expanding landscape of moonlighting proteins in yeasts. *Microbiol Mol Biol Rev* **80**, 765-77. https://doi.org/10.1128/MMBR.00012-16

Gebicka, L., Didik, J. (2009) Catalytic scavenging of peroxynitrite by catalase. *J Inorg Biochem* **103**, 1375-9. https://doi.org/10.1016/j.jinorgbio.2009.07.011

Geer, B.W., Krochko, D., Oliver, M.J., Walker, V.K., Williamson, J.H. (1980) A comparative study of the NADP-malic enzymes from Drosophila and chick liver. *Comp Biochem Physiol* **65**, 25-34. https://doi.org/10.1016/0305-0491(80)90109-1

Gounaris, A.D., Turkenkopf, I., Buckwald, S., Young, A. (1971) Pyruvate decarboxylase. I. Protein dissociation into subunits under conditions in which thiamine pyrophosphate is released. *J Biol Chem* 246, 1302-9. https://doi.org/10.1016/S0021-9258(19)76974-9

Horan, S., Bourges, I., Meunier, B. (2006) Transcriptional response to nitrosative stress in *Saccharomyces cerevisiae*. *Yeast* **23**, 519-35. https://doi.org/10.1002/yea.1372

Jahnová, J., Luhová, L., Petřivalský, M. (2019) S-nitrosoglutathione reductase-the master regulator of protein s-nitrosation in plant NO signaling. *Plants (Basel)* **8**, 48. https://doi.org/10.3390/plants8020048

Kalinina, E., Novichkova, M. (2021) Glutathione in protein redox modulation through S-glutathionylation and S-Nitrosylation. *Molecules* **26**, 435. https://doi.org/10.3390/molecules26020435

Kitichantaropas, Y., Boonchird, C., Sugiyama, M., Kaneko, Y., Harashima, S., Auesukaree, C. (2016) Cellular mechanisms contributing to multiple stress tolerance in *Saccharomyces cerevisiae* strains with potential use in high-temperature ethanol fermentation. *AMB Express* **6**, 107. https://doi.org/10.1186/s13568-016-0285-x

Kruf, C., Nookaew, I., Brown, S.H., McCulloch, M., Berry, A., Nielsen, J. (2013) Investigation of malic acid production in *Aspergillus oryzae* under nitrogen starvation conditions. *Appl Environ Microbiol* **79**, 6050-8. https://doi.org/10.1128/AEM.01445-13

Kurutas, E.B. (2016) The importance of antioxidants which play the role in cellular response against oxidative/nitrosative stress: current state. *Nutr J* **15**, 71. https://doi.org/10.1186/s12937-016-0186-5

Laemmli, U.K. (1970) Cleavage of structural proteins during the assembly of the head of bacteriophage T4. *Nature* **227**, 680-5. https://doi.org/10.1038/227680a0

Lei, X.G., Zhu, J.H., Cheng, W.H., Bao, Y., Ho, Y.S., Reddi, A.R., Holmgren, A., Arnér, E.S. (2016) Paradoxical roles of antioxidant enzymes: basic mechanisms and health implications. *Physiol Rev* **96**, 307-64. https://doi.org/10.1152/physrev.00010.2014

Lindemann, C., Lupilova, N., Müller, A., Warscheid, B., Meyer, H.E., Kuhlmann, K., Eisenacher, M., Leichert, L.I. (2013) Redox proteomics uncovers peroxynitrite-sensitive proteins that help *Escherichia coli* to overcome nitrosative stress. *J Biol Chem* **288**, 19698-714. https://doi.org/10.1074/jbc.M113.457556

Liu, L., Zeng, M., Hausladen, A., Heitman, J., Stamler, J.S. (2000) Protection from nitrosative stress by yeast flavohemoglobin. *Proc Natl Acad Sci USA* **97**, 4672-6. https://doi.org/10.1073/pnas.090083597

Lushchak, O.V., Inoue, Y., Lushchak, V.I. (2010) Regulatory protein Yap1 is involved in response of yeast *Saccharomyces cerevisiae* to nitrosative stress. *Biochem (Mosc)* **75**, 629-64. https://doi.org/10.1134/s0006297910050135

Lushchak, O.V., Piroddi, M., Galli, F., Lushchak, V.I. (2014) Aconitase post-translational modification as a key in linkage between Krebs cycle, iron homeostasis, redox signaling, and metabolism of reactive oxygen species. *Redox Rep* **19**, 8-15. https://doi.org/10.1179/1351000213Y.0000000073

Maciejczyk, M., Zalewska, A., Gryciuk, M., Hodun, K., Czuba, M., Płosaczyca, K., Charmas, M., Sadowski, J., Baranowski, M. (2022) Effect of Normobaric Hypoxia on Alterations in Redox Homeostasis, Nitrosative Stress, Inflammation, and Lysosomal Function following Acute Physical Exercise. *Oxid Med Cell Longev* **2022**, 4048543. https://doi.org/10.1155/2022/4048543

Maestre, O., García-Martínez, T., Peinado, R.A., Mauricio, J.C. (2008) Effects of *ADH2* overexpression in *Saccharomyces bayanus* during alcoholic fermentation. Appl Environ Microbiol. **74,** 702-7. https://doi.org/10.1128/AEM.01805-07

Mithra, M.G., Jeeva, M.L., Sajeev, M.S., Padmaja, G. (2018) Comparison of ethanol yield from pretreated lignocellulo-starch biomass under fed-batch SHF or SSF modes. *Heliyon* **4,** e00885. https://doi.org/10.1016/j.heliyon.2018.e00885

Miyagi, H., Kawai, S., Murata, K. (2009) Two sources of mitochondrial NADPH in the yeast Saccharomyces cerevisiae. *J Biol Chem* **284**, 7553-60. https://doi.org/10.1074/jbc.M804100200

Nasuno, R., Aitoku, M., Manago, Y., Nishimura, A., Sasano, Y., Takagi, H. (2014) Nitric oxide-mediated antioxidative mechanism in yeast through the activation of the transcription factor Mac1. *PLoS One* **9**, e113788. https://doi.org/10.1371/journal.pone.0113788

Navarro, M.V., Chaves, A.F.A., Castilho, D.G., Casula, L., Calado, J.C.P., Conceição, P.M., Iwai, L.K., de Castro, B.F., Batista, W.L. (2020) Effect of nitrosative stress on the *s*-nitroso-proteome of *Paracoccidioides brasiliensis*. *Front Microbiol* **11**, 1184. https://doi.org/10.3389/fmicb.2020.01184

Patra, S.K., Bag, P.K., Ghosh, S. (2017) Nitrosative Stress Response in *Vibrio cholerae*: Role of S-Nitrosoglutathione Reductase. *Appl Biochem Biotechnol* **182**, 871-884. https://doi.org/10.1007/s12010-016-2367-2

Patra, S.K., Samaddar, S., Sinha, N., Ghosh, S. (2019) Reactive nitrogen species induced catalases promote a novel nitrosative stress tolerance mechanism in *Vibrio cholerae*. *Nitric Oxide* **88**, 35-44. https://doi.org/10.1016/j.niox.2019.04.002

Payne, J., Morris, J.G. (1969) Pyruvate carboxylase in *Rhodopseudomonas spheroides*. *J Gen Microbiol* **59**, 97-101. https://doi.org/10.1099/00221287-59-1-97

Peláez-Soto A, Roig P, Martínez-Culebras PV, Fernández-Espinar MT, Gil JV (2020) Proteomic analysis of *Saccharomyces cerevisiae* response to oxidative stress mediated by cocoa polyphenols extract. *Molecules* **25**, 452. https://doi.org/10.3390/molecules25030452

Peluffo, G., Radi, R. (2007) Biochemistry of protein tyrosine nitration in cardiovascular pathology. *Cardiovasc Res* **75**, 291-302. https://doi.org/10.1016/j.cardiores.2007.04.024

Pfeiffer, T., Morley, A. (2014) An evolutionary perspective on the Crabtree effect. *Front Mol Biosci* **1**, 17. https://doi.org/10.3389/fmolb.2014.00017

Pollak, N., Dölle, C., Ziegler, M. (2007) The power to reduce: pyridine nucleotides--small molecules with a multitude of functions. *Biochem J* **402**, 205-18. https://doi.org/10.1042/BJ20061638

Radi, R. (2018) Oxygen radicals, nitric oxide, and peroxynitrite: Redox pathways in molecular medicine. *Proc Natl Acad Sci USA* **115**, 5839-5848. https://doi.org/10.1073/pnas.1804932115

Redzepovic, S., Orlic, S., Majdak, A., Kozina, B., Volschenk, H., Viljoen-Bloom, M. (2003) Differential malic acid degradation by selected strains of Saccharomyces during alcoholic fermentation. *Int J Food Microbiol* **83**, 49-61. https://doi.org/10.1016/s0168-1605(02)00320-3

Regev-Shoshani, G., Crowe, A., Miller, C.C. (2013) A nitric oxide-releasing solution as a potential treatment for fungi associated with tinea pedis. *J Appl Microbiol* **114**, 536-44. https://doi.org/10.1111/jam.12047

Remize, F., Andrieu, E., Dequin, S. (2000) Engineering of the pyruvate dehydrogenase bypass in Saccharomyces cerevisiae: role of the cytosolic Mg(2+) and mitochondrial K(+) acetaldehyde dehydrogenases Ald6p and Ald4p in acetate formation during alcoholic fermentation. *Appl Environ Microbiol* **66**, 3151-9. https://doi.org/10.1128/AEM.66.8.3151-3159.2000

Ridnour, L.A., Thomas, D.D., Mancardi, D., Espey, M.G., Miranda, K.M., Paolocci, N., Feelisch, M., Fukuto, J., Wink, D.A. (2004) The chemistry of nitrosative stress induced by nitric oxide and reactive nitrogen oxide species. Putting perspective on stressful biological situations. *Biol Chem* **385**, 1-10. https://doi.org/10.1515/BC.2004.001

Saboo, R., Bhattacharjee, A., Majumdar, U., Ray, S.S., Dutta, T., Ghosh, S. (2009) A novel role of catalase in detoxification of peroxynitrite in *S. cerevisiae*. *Biochem Biophys Res Commun* **385**, 507-11. https://doi.org/10.1016/j.bbrc.2009.05.062

Saboo, R., Dutta, T., Das, A., Sinha Ray, S., Sengupta, R., Ghosh, S. (2006) Effect of nitrosative stress on Schizosaccharomyces pombe: inactivation of glutathione reductase by peroxynitrite. Free Radic Biol Med **40**, 625–631. https://doi.org/10.1016/j.freeradbiomed.2005.09.029

Saboo, R., Sengupta, R., Ghosh, S. (2003) Nitrosative stress on yeast: inhibition of glyoxalase-I and glyceraldehyde-3-phosphate dehydrogenase in the presence of GSNO. *Biochem Biophys Res Commun* **302**, 665-70. https://doi.org/10.1016/s0006-291x(03)00251-1

Sengupta, S., Deb, M., Nath, R., Saha S.P., Bhattacharjee, A. (2020) Optimization of ethanol production using nitrosative stress exposed *S. cerevisiae*. *Cell Biochem Biophys* **78**, 101-110. https://doi.org/10.1007/s12013-019-00897-y

Shannon, P., Markiel, A., Ozier, O., Baliga, N.S., Wang, J.T., Ramage, D., Amin, N., Schwikowski, B., Ideker, T. (2003) Cytoscape: a software environment for integrated models of biomolecular interaction networks. *Genome Res* **13**, 2498-504. https://doi.org/10.1101/gr.1239303

Sies, H., Sharov, V.S., Klotz, L.O., Briviba, K. (1997) Glutathione peroxidase protects against peroxynitrite-mediated oxidations. A new function for selenoproteins as peroxynitrite reductase. *J Biol Chem* **272**, 27812-7. https://doi.org/10.1074/jbc.272.44.27812

Srere, P.A. (1969) Citrate synthase: [EC 4.1.3.7. Citrate oxaloacetate-lyase (CoA-acetylating)]. *Methods Enzymol* **13**, 3-11. https://doi.org/10.1016/0076-6879(69)13005-0

Staab, C.A., Alander, J., Brandt, M., Lengqvist, J., Morgenstern, R., Grafström, R.C., Höög, J.O. (2008) Reduction of S-nitrosoglutathione by alcohol dehydrogenase 3 is facilitated by substrate alcohols via direct cofactor recycling and leads to GSH-controlled formation of glutathione transferase inhibitors. *Biochem J* **413**, 493-504. https://doi.org/10.1042/BJ20071666

Szklarczyk, D., Gable, A.L., Lyon, D., Junge, A., Wyder, S., Huerta-Cepas, J., Simonovic, M., Doncheva, N.T., Morris, J.H., Bork, P., Jensen, L.J., Mering, C.V. (2019) STRING v11: protein-protein association networks with increased coverage, supporting functional discovery in genome-wide experimental datasets. *Nucleic Acids Res* **47**, D607-D613. https://doi.org/10.1093/nar/gky1131

Tillmann, A., Gow, N.A., Brown, A.J. (2011) Nitric oxide and nitrosative stress tolerance in yeast. *Biochem Soc Trans* **39**, 219-23. https://doi.org/10.1042/BST0390219

Voet, D. and Voet, J.G. (1995) Biochemistry. J. Wiley & Sons, New York

Wachnowsky, C., Hendricks, A.L., Wesley, N.A., Ferguson, C., Fidai, I., Cowan, J.A. (2019) Understanding the mechanism of [4Fe-4S] cluster assembly on eukaryotic mitochondrial and cytosolic aconitase. *Inorg Chem* **58**, 13686-95. https://doi.org/10.1021/acs.inorgchem.9b01278

Wang, Y.T., Piyankarage, S.C., Williams, D.L., Thatcher, G.R. (2014) Proteomic profiling of nitrosative stress: protein S-oxidation accompanies S-nitrosylation. *ACS Chem Biol* **9**, 821-30. https://doi.org/10.1021/cb400547u

Witkiewicz-Kucharczyk, A., Goch, W., Okędzki, J., Hartwig, A., Bal, W. (2020) The reactions of H_2O_2 and GSNO with the zinc finger motif of XPA. Not a regulatory mechanism, but no synergy with cadmium toxicity. *Molecules* **25**, 4177. https://doi.org/10.3390/molecules25184177

Xiao, W., Wang, R.S., Handy, D.E., Loscalzo, J. (2018) NAD(H) and NADP(H) redox couples and cellular energy metabolism. *Antioxid Redox Signal* **28**, 251-272. https://doi.org/10.1089/ars.2017.7216

Yazgan, O., Krebs, J.E. (2012) Mitochondrial and nuclear genomic integrity after oxidative damage in Saccharomyces cerevisiae. *Front Biosci (Landmark Ed)* **17**, 1079-93. https://doi.org/10.2741/3974

Ying, T., Jinsong, G., Dong, W., Kaike, W., Jue, Z., Jing, F. (2017) The potential regulatory effect of nitric oxide in plasma activated water on cell growth of *Saccharomyces cerevisiae*. *J Appl Phys* **122**, 123302. https://doi.org/10.1063/1.4989501

Yoshikawa, Y., Nasuno, R., Kawahara, N., Nishimura, A., Watanabe, D., Takagi, H. (2016) Regulatory mechanism of the flavoprotein Tah18-dependent nitric oxide synthesis and cell death in yeast. *Nitric Oxide* **57**, 85-91. https://doi.org/10.1016/j.niox.2016.04.003

Zhang, P., Hai, H., Su, D., Yuan, W., Liu, W., Ding, R., Teng, M., Ma, L., Tian, J., Chen, C. (2019) A high throughput method for total alcohol determination in fermentation broths. *BMC biotechnol* **19**, 30. https://doi.org/10.1186/s12896-019-0525-7

Figure captions

Fig. 1 Effect of 0.5 mM acidified sodium nitrite on **(A)** GSH/GSSG ratio, **(B)** specific activity of glutathione reductase, and catalase. Data are expressed as the change in the percentage of specific activity as compared to the control. Assays were performed in triplicate for each biological sample and expressed as mean±SD. White and black bars represent control and ac.$NaNO_2$-treated cells, respectively.

Fig. 2 Effect of 0.5 mM acidified sodium nitrite on reactive nitrogen species and reactive oxygen species generation. Confocal microscopy analysis for the generation of reactive nitrogen species **(A-D)** and reactive oxygen species **(F-I)**. Micrographs were recorded at 45X magnification. Bar=100 µm. The mean fluorescent intensity for reactive nitrogen species **(E)** and reactive oxygen species **(J)** were determined by using Leica LAS X software and represented as mean±SD. FACS analysis for the reactive nitrogen species **(K, L)** and reactive oxygen species **(M, N)**. FACS analysis was done by using FACS Diva software.

Fig. 3 Effect of 0.5 mM acidified sodium nitrite on **(A)** the specific activity of various relevant enzymes. Data are expressed as the change in the percentage of specific activity as compared to the control. **(B)** Citrate content of extracellular and intracellular fractions combined. Assays were done in triplicate and represented as mean±SD. White and black bars represent control and ac.$NaNO_2$-treated cells, respectively.

Fig. 4 Network representation of enzymes in the presence of 0.5 mM acidified sodium nitrite. Network representation of **(A)** enzymes with increased activities and **(B)** enzymes with decreased activities. Highlighted colour denotes the enzymes with experimentally validated activities.

Fig. 5 Effect of 0.5 mM acidified sodium nitrite on three *ADH* and two *ACO* genes. The expression level of the genes was normalized with that of *GAPDH* (glyceraldehyde-3-phosphate dehydrogenase) in each set and expressed as the relative fold change as compared to the control. White and black bars represent control and ac.$NaNO_2$-treated cells, respectively.

Fig. 6 Effect of different concentrations of acidified sodium nitrite (0.1, 0.3, 0.5 mM) and 0.1 mM peroxynitrite on the specific activity of pure proteins (aconitase and alcohol dehydrogenase) along with the protein tyrosine nitration (PTN) formation. Western blotting for PTN and specific activity of **(A)** aconitase, **(B)** alcohol dehydrogenase. Data are expressed in A and B as the change in the percentage of specific activity as compared to the control. The assays were performed in triplicate and expressed as mean±SD.

Fig. 7 Proposed switching of glucose metabolism in the presence of 0.5 mM acidified sodium nitrite. Green downward arrows represent upregulated enzymes and red upward arrows represent downregulated enzymes in the presence of 0.5 mM acidified sodium nitrite. In this condition, energy generation through TCA cycle was compromised due to the lower activity of pyruvate dehydrogenase (PDH), citrate synthase (CS), aconitase (ACO), isocitrate dehydrogenase (ICDH), pyruvate carboxylase (PC) but the glucose metabolic flux was rerouted via higher activity of malate dehydrogenase (MDH) and malate dehydrogenase (decarboxylating) [MDH(DC)] towards pyruvate which was further metabolized via the fermentative pathway with the help of higher activity of pyruvate decarboxylase (PDC) and alcohol dehydrogenase (ADH) which resulted in higher production of ethanol. In addition, activity of malate synthase (MS) and aldehyde dehydrogenase (ALDH) were reduced that might affect the glyoxylate shunt (an anaplerotic variant of TCA cycle) and PDH-bypass pathway (an alternative route of acetyl-CoA synthesis without the activity of PDH).

Table 1 Estimation of ethanol concentration, glucose consumption, ethanol yield, percentage of theoretical yield and volumetric productivity of treated and untreated (control) samples of *S. cerevisiae*

Sample	Ethanol concentration (g/L)	Glucose consumed (g/L)	Ethanol yield (g/g of glucose)	% of theoretical yield	Volumetric Productivity (g/L/h)
Control	4.5±0.3	15±0.3	0.30	59	0.38
Treated	6±0.5	17±0.4	0.35	69	0.50

Table 2 Functional enrichment by activation/ deactivation of enzymes

	Term	% of genes	P-Value	Benjamini adjusted P-Value
Enrichment by activated enzymes due to stress				
Biological Process	pyruvate metabolic process	31.6	3.8E-10	8.7E-9
	malate metabolic process	26.3	3.8E-10	8.7E-9
	Fermentation	10.5	9.7E-3	4.0E-2
Cellular Components	mitochondrial matrix	31.6	3.1E-5	4.1E-4
	cytosol	42.1	2.1E-2	9.0E-2
Molecular Function	malate dehydrogenase activity	15.8	3.8E-5	6.1E-4
	alcohol dehydrogenase (NAD) activity	15.8	1.9E-4	2.3E-3
	Pyruvate kinase activity	26.3	3.6E-4	3.5E-3
Enrichment by deactivated enzymes due to stress				
Biological Process	tricarboxylic acid cycle	38.5	2.8E-15	1.5E-13
	glyoxylate cycle	19.2	6.6E-8	1.2E-6
	acetate biosynthetic process	11.5	1.2E-4	9.1E-4
Cellular Components	Peroxisomal matrix	42.3	4.3E-11	9.0E-10
	mitochondrial nucleoid	15.4	1.3E-4	9.2E-4
Molecular Function	aldehyde dehydrogenaseactivity	19.2	1.7E-7	9.3E-6
	transferase activity, transferring acyl groups, acyl groups converted into alkyl on transfer	15.4	9.8E-6	1.3E-4
	lyase activity	23.1	1.1E-4	9.7E-4

Figure 1

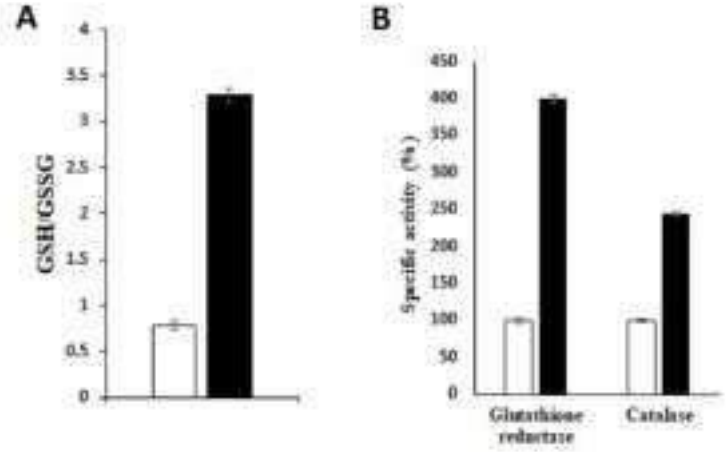

Figure 2

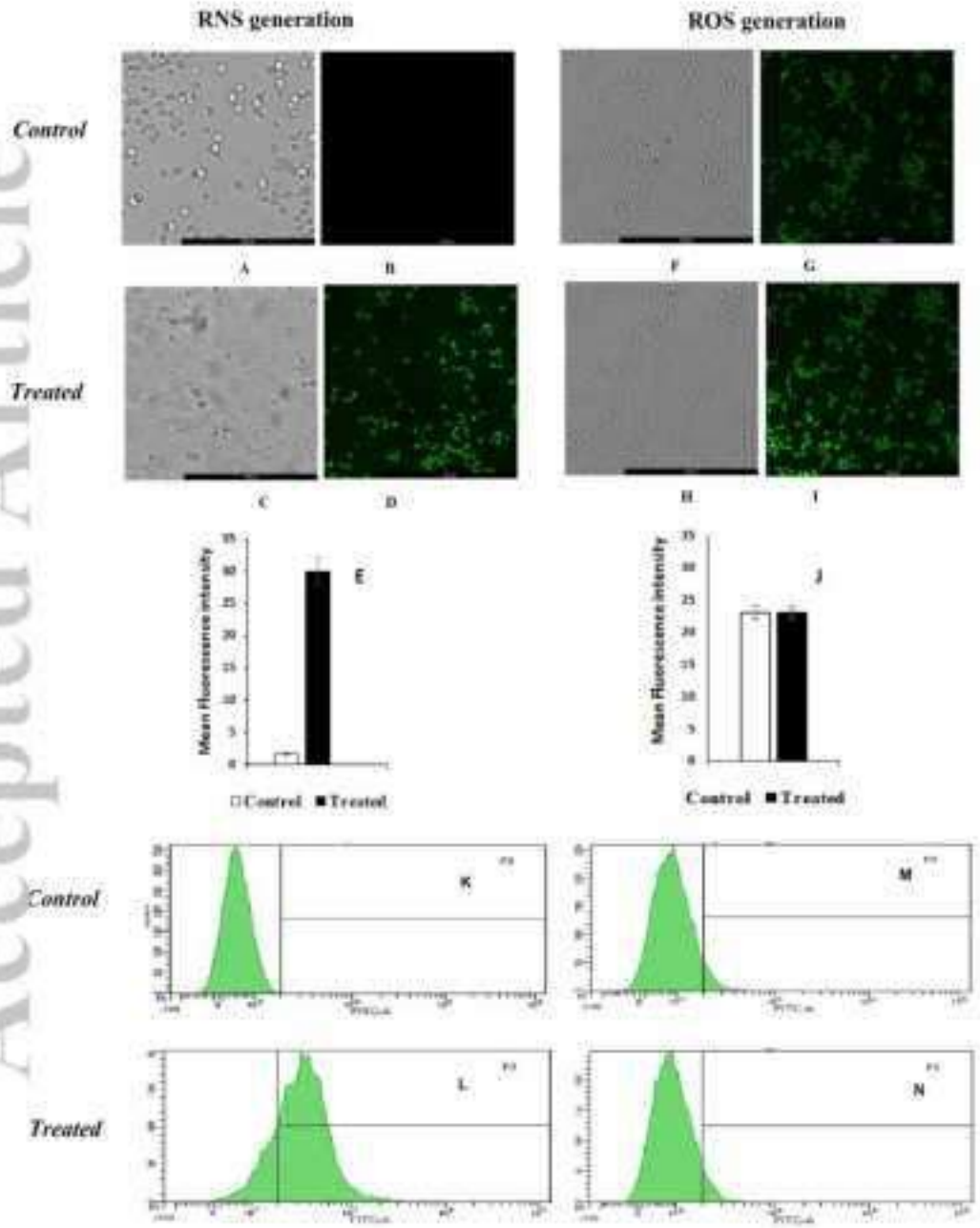

Figure 3

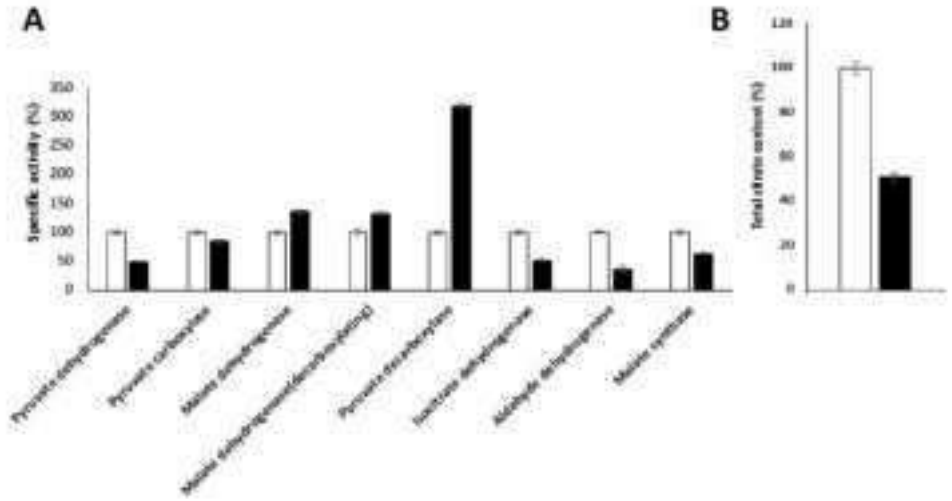

Figure 4

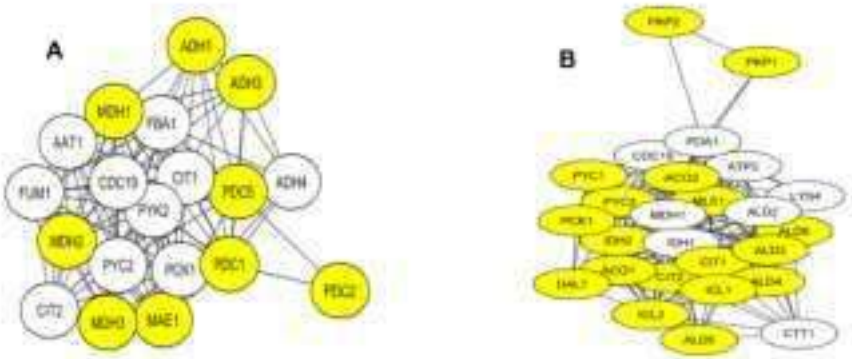

Figure 5

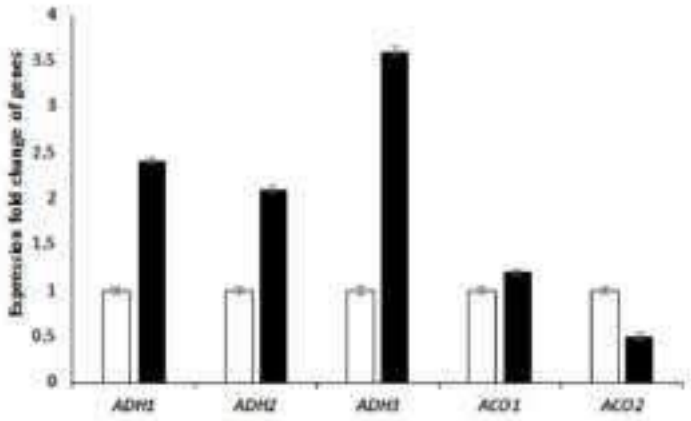

Figure 6

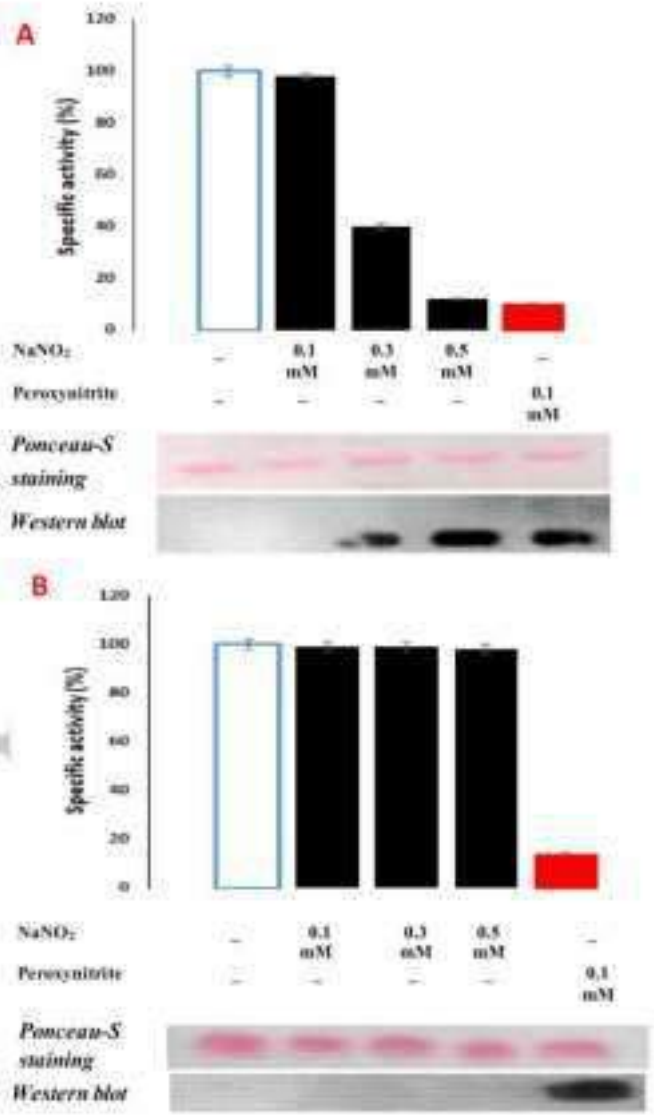

Figure 7

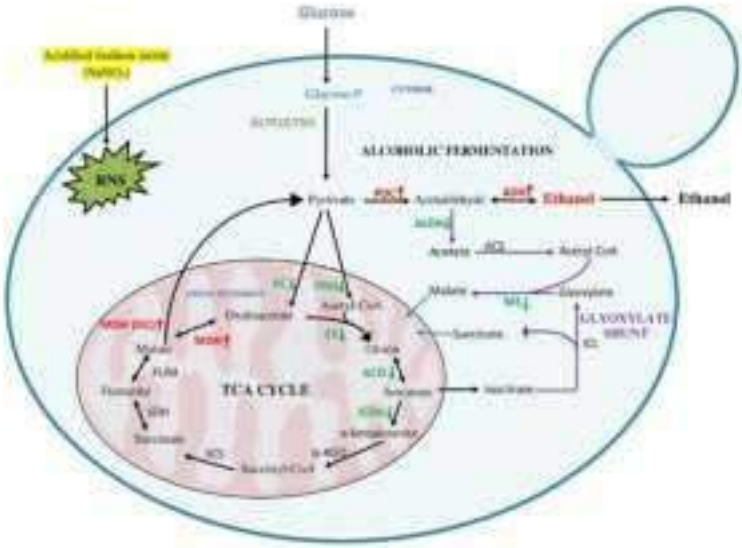

Seminars...

1st Regional Science and Technology Congress-2016
Jalpaiguri Division, West Bengal

Organized by

Department of Science & Technology, Government of West Bengal

&

Ananda Chandra College, Jalpaiguri

Outstanding Paper Award

is presented to

Swarnab Sengupta

for the paper co-authored with

Arindam Bhattacharjee

titled

Characterizing the effect of nitrosative stress on ethanol production by Saccharomyces cerevisiae

presented at

Ananda Chandra College, Jalpaiguri on November 7-8, 2016

Sonam Yogel Bhutia
Nodal Officer
1st Regional Science and
Technology Congress-2016
Jalpaiguri Division, West Bengal

Dr. Dhiraj Kumar Basak
Principal
Ananda Chandra College
Jalpaiguri

Arvind Kumar Mina, IAS
Joint Secretary
Department of Science and Technology
Government of West Bengal

International Conference on Nanotechnology: Ideas, Innovations and Initiatives – 2017 (ICN:3I-2017)

Organized by

Dept. of Mechanical & Industrial Engineering and Centre of Nanotechnology

Certificate of Appreciation

ICN:3I-2017 is pleased to award this certificate to

Prof./Dr./Ms./Mr. Suvarnali Sengupta

from University of North Bengal, Siliguri, India

for presenting ~~Plenary~~ / ~~Invited~~ / Oral / ~~Poster~~ / ~~Participation~~ in this International Conference held at Indian Institute of Technology, Roorkee, India during 06-08 December 2017.

Dr. Kaushik Pal	Prof. Sumeer K. Nath	Prof. Dinesh Kumar
Convener, ICN:3I-2017	Chairman, ICN:3I-2017	Chairman, ICN:3I-2017

An Interdisciplinary National Seminar

Vistas in Life Science Research

March 29, 2019

Organized by

Department of Biotechnology, Department of Microbiology,
Department of Tea Science & Department of Bioinformatics

University of North Bengal

Accredited by NAAC with grade A

CERTIFICATE OF PARTICIPATION

Prof/Dr/Mr/Ms. SWARNAB SENGUPTA *participated as a registered delegate in the seminar. He / She presented paper on* 'BEST ORAL PRESENTATION' ..... *in the invited/oral/poster session and chaired the session* TECHNICAL SESSION

Dipanwita Saha

Dr. Dipanwita Saha
Organizing Secretary

Prof. Pranab Ghosh
Chairman